Regulation of Ephrin-A Expression in Compressed Retinocollicular Maps

Tizeta Tadesse,[1,2]* Qi Cheng,[1]*† Mei Xu,[2]*‡ Deborah J. Baro,[1,2] Larry J. Young,[3] Sarah L. Pallas[1,2]

[1] Neuroscience Institute, Georgia State University, Atlanta, Georgia

[2] Department of Biology, Graduate Program in Neurobiology & Behavior, Georgia State University, Atlanta, Georgia

[3] Center for Translational Social Neuroscience, Department of Psychiatry and Behavioral Sciences, Yerkes National Primate Research Center, Emory University, Atlanta Georgia

Received 5 June 2012; revised 14 September 2012; accepted 18 September 2012

ABSTRACT: **Retinotopic maps can undergo compression and expansion in response to changes in target size, but the mechanism underlying this compensatory process has remained a mystery. The discovery of ephrins as molecular mediators of Sperry's chemoaffinity process allows a mechanistic approach to this important issue. In Syrian hamsters, neonatal, partial (PT) ablation of posterior superior colliculus (SC) leads to compression of the retinotopic map, independent of neural activity. Graded, repulsive EphA receptor/ephrin-A ligand interactions direct the formation of the retinocollicular map, but whether ephrins might also be involved in map compression is unknown. To examine whether map compression might be directed by changes in the ephrin expression pattern, we compared ephrin-A2 and ephrin-A5 mRNA expression between normal SC and PT SC using *in situ* hybridization and quantitative real-time PCR. We found that ephrin-A ligand expression in the compressed maps was low anteriorly and high posteriorly, as in normal animals. Consistent with our hypothesis, the steepness of the ephrin gradient increased in the lesioned colliculi. Interestingly, overall levels of ephrin-A2 and -A5 expression declined immediately after neonatal target damage, perhaps promoting axon outgrowth. These data establish a correlation between changes in ephrin-A gradients and map compression, and suggest that ephrin-A expression gradients may be regulated by target size. This in turn could lead to compression of the retinocollicular map onto the reduced target. These findings have important implications for mechanisms of recovery from traumatic brain injury.** Develop Neurobiol 73: 274–296, 2013

Keywords: **retinotectal; population matching; topographic map; axon guidance; neural plasticity**

*These authors contributed equally to this study.

†*Present address:* Department of Human Genetics, Emory University Medical School, Atlanta, GA, USA.

‡*Present address:* Philadelphia College of Osteopathic Medicine, Anatomy, Philadelphia, Pennsylvania, USA.

Correspondence to: S.L. Pallas (spallas@gsu.edu).

Contract grant sponsor: NIH; contract grant numbers: EY-12696 (to S.L.P.), NSF 0078110 (to S.L.P.).

Contract grant sponsor: NSF; contract grant number: STC IBN-9876754 (to L.J.Y.).

Contract grant sponsor: NIH; contract grant number: NS-38770 (to D.J.B.).

Contract grant sponsor: GSU Research Foundation (to S.L.P. and D.J.B.).

Published online 25 September 2012 in Wiley Online Library (wileyonlinelibrary.com).
DOI 10.1002/dneu.22059

INTRODUCTION

Topographic maps are an important organizational feature of nervous systems, and the retinotectal projection of vertebrates has long been the system of choice for studying the mechanisms underlying map formation. Roger Sperry's classic experiments on amphibians suggested that regenerating retinal axons follow matching "chemoaffinity" markers in the tectum (Sperry, 1963). Consistent with this idea, retinal axons regenerating from ventral half-eyes initially innervate only dorsal tectum (Schmidt et al., 1978). Similarly, half-tecta are initially innervated only by the corresponding half of the retina (Attardi and Sperry, 1963). Contrary to Sperry's interpretation, however, the maps eventually regulate such that the retinal axons occupy all of the available target space, creating an expanded or compressed retinotectal map of visual space (Gaze and Sharma, 1970; Yoon, 1976; Schmidt, 1983; see Schmidt, 1982, for review). Compression of retinal maps has also been shown to occur in mammals after half-tectal ablations performed during development (Finlay et al., 1979), providing a model for investigation of the mechanisms underlying developmental plasticity of retinotopic maps (Pallas and Finlay, 1989, 1991; Xiong et al., 1994; Huang and Pallas, 2001; Razak and Pallas, 2007).

It has been suggested that reorganization of chemoaffinity markers is necessary for topographic map plasticity to occur (Schmidt, 1978; Willshaw and Von Der Malsburg, 1979; Feldheim et al., 2000; Willshaw, 2006) but a direct test of this hypothesis has been lacking. An alternative hypothesis is that competition between retinal axons, in addition to existing chemoaffinity cues, is sufficient to reorganize the map (Triplett et al., 2011). Although some evidence from zebrafish argues against competition as a critical factor in development of at least some aspects of normal maps (Gosse and Baier, 2009), plasticity in maps may rely on interaxonal competition. The aim of this study was to investigate the role of chemoaffinity markers in map compression during developmental plasticity.

Multiple studies across several species support the idea that graded distribution of ephrins and their receptors comprise the chemoaffinity markers that Sperry proposed, although the mechanism by which they direct retinotopic map formation is only partially understood (Walter et al., 1987a,b; Ciossek et al., 1998; Feldheim et al., 2000; Mortimer et al., 2010; Gebhardt et al., 2012; see Triplett and Feldheim, 2012, for review). Whether ephrins might direct injury-induced changes in retinotopy such as map compression is unknown, although there is evidence for their involvement in regeneration (Rodger et al., 2005). Previous *in vitro* work has shown that both the slope of the gradient and local, relative concentration differences in ephrin-A expression are important for axon guidance (Rosentreter et al., 1998; Brown et al., 2000; Reber et al., 2004; von Philipsborn et al., 2006). Based on this body of data, we hypothesized that retinotectal map compression is directed by injury-induced alterations in ephrin concentration gradients. If so, then this could be manifested through increases in gradient steepness in lesioned animals.

In order to test the prediction that map compression would be associated with compression of ephrin gradients (Fig. 1), we induced retinotectal (retinocollicular) map compressions in Syrian hamsters by ablation of the posterior part of the superficial SC at birth (Finlay et al., 1979; Wikler et al., 1986; Pallas and Finlay, 1989). The spatial patterns of expression of ephrin-A2 and -A5 were analyzed using *in situ* hybridization. For quantitative measurements of expression, quantitative real-time PCR was employed. We report here that ephrin gradients were steeper in compressed maps, providing support for the hypothesis that gradient compression is responsible for map compression. These data complement previous *in vitro* studies regarding how ephrin-A ligands guide retinotectal axons. They are important in providing a window into the role of ephrin-A ligands in the *in vivo* behavior of axons in normal development and in developmental plasticity after traumatic brain injury.

METHODS

Animals

Syrian hamsters (*Mesocricetus auratus*) at different postnatal ages were used (postnatal day (P) 1, 3, 4, 5, 6, 8, 12, and 14; the first 24 h after birth is considered P0) (Table 1). Hamsters were chosen as a model because their retinal axons have not yet arborized in the SC at birth (Frost et al., 1979), because their SC visual physiology has been well-characterized (Tiao and Blakemore, 1976; Chalupa and Rhoades, 1977; Finlay et al., 1978; Stein and Dixon, 1979), and because our previous studies of retinocollicular map plasticity were performed in this species (Pallas and Finlay, 1989; Huang and Pallas, 2001; Razak et al., 2003). Normal and experimental animals were bred in the Georgia State University animal facility. Breeding stock were either purchased from Charles River Laboratories (Wilmington, MA) or obtained from descendants of a wild-caught population (Gattermann et al., 2000; Fritzsche et al., 2006). All of the

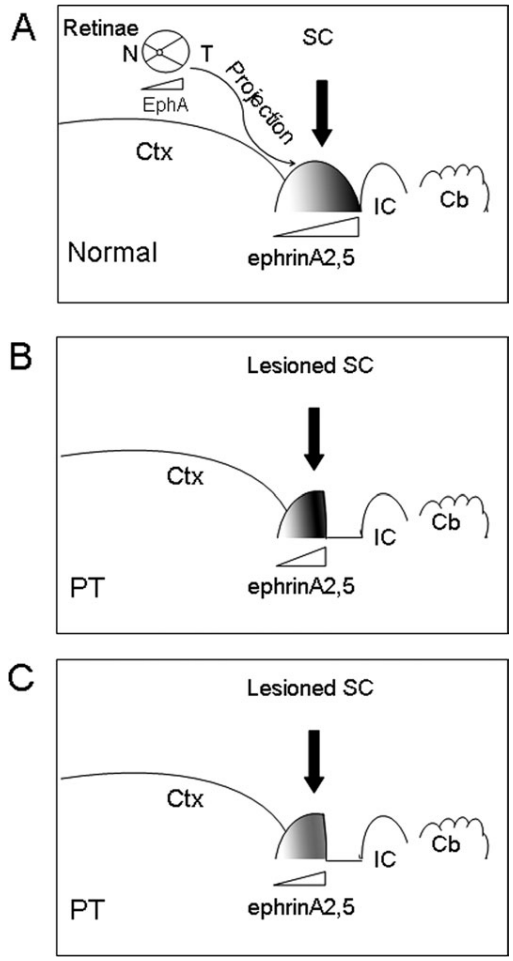

Figure 1 Alternate hypotheses: expression of ephrin-A ligands in compressed retinocollicular maps. Schematic representation of retinal ganglion cell projections to the SC under the guidance of EphA receptors on retinal axons and their ephrin ligands in (A) Normal and (B, C) partially ablated (PT) SC. Ablations were always posterior. (A) EphA receptors are normally expressed in a low nasal, high temporal gradient in retina, whereas ephrin-A2 and -A5 ligands are expressed in a low anterior to high posterior gradient in SC. (B and C) Partial ablation of posterior SC on the day of birth is indicated. (B) If the steepness of ephrin-A2 and -A5 gradients instructs targeting specificity, then the steepness should increase in compressed maps. (C) Alternatively, if only the relative steepness of the gradient is important, then the steepness need not change in compressed maps. (SC, superior colliculus, A, anterior, P, posterior, T, temporal, N, nasal).

animal procedures used here met or exceeded the standards for humane care set by the Society for Neuroscience and the National Institutes of Health and were approved by the Institutional Animal Care and Use Committee at Georgia State University.

Neonatal Surgery

Partial (PT) SC ablation surgery within 12 h of birth reliably results in compression of the retinocollicular map, as long as the lesions eliminate less than 70% of the posterior SC, in which case a partial map is formed (Finlay et al., 1979; Wikler et al., 1986; Pallas and Finlay, 1989). At birth in Syrian hamsters retinal axons have grown a little more than halfway to the posterior edge of the SC but have made few if any synapses (Frost et al., 1979). The PT ablation of posterior SC may thus damage some of the growing axons that then regenerate, and they along with undamaged axons that grow in later create the compressed retinotopic map on the reduced SC. The procedure causes only a slight increase in the amount of natural cell death in the SC neuron population (Wikler et al., 1986) and synaptic density within SC remains the same (Xiong and Finlay, 1993), thus for a 50% ablation approximately twice as many retinal ganglion cells are available to each SC neuron.

To perform PT SC ablation, a surgical plane of anesthesia was induced with 4% isoflurane in 0.5 L/min oxygen, and was maintained with 1 to 2% isoflurane. An incision over the midbrain was made, exposing the thin skull through which the SC could be seen. The superficial layer of the posterior half of the right SC was ablated using a cautery tip applied briefly to the skull. The wound was closed using 6-0 silk suture or Vetbond© (3M, St. Paul, MN) and the pups were returned to the mother. Sham surgery (duplicating the surgical procedure but without use of the cautery) was performed on three animals to control for any effects of the anesthesia and handling on ephrin expression. Tissue from the sham surgery animals was analyzed at P5 only. Lesion sizes were evaluated either through reconstruction of adjacent Nissl sections in the case of brains used for *in situ* hybridization, or by direct visual inspection of the whole brain before homogenization, in the case of brains used for qRT-PCR.

Cloning of Hamster Ephrin-A2 and A5

Total RNA was isolated from Syrian hamster diencephalon and mesencephalon using Trizol (Invitrogen, Carlsbad, CA). SuperScript II (Invitrogen, Carlsbad, CA) was used to synthesize cDNA from RNA through a reverse transcription polymerase chain reaction (RT-PCR) using degenerate oligonucleotide primers based on mammalian sequences. Lasergene software (DNA Star, Madison, WI) was used to select degenerate primer pairs from conserved regions of human and mouse sequences published at Genbank, and primer pairs were then custom-synthesized (Invitrogen, Carlsbad, CA). The oligonucleotide primers were as follows: ephrin-A2: forward 5'-GGCCCGGGCCAACGCTGACCGATAC-3'; reverse 5'-CCAGGCCGGAACTCAAAGCCCAGGGAAAAG-3'. Ephrin-A5: forward 5'-ATGTTGACGCTGCTCTTTCTGGTGCTCTGG-3'; reverse 5'-GGCGGCTGGGTATCCTTGGTGTCTGC-3'.

Expected PCR products were 348 base pairs for ephrin-A2 and 544 base pairs for ephrin-A5. Ephrin-A2 PCR

Table 1 Syrian Hamster Pups used for *In Situ* Hybridization and Quantitative Real-Time PCR

	No. Normal Animals		No. Half-SC Normals		No. Sham Operates	No. PT Animals	
Postnatal Age (P)	ISH	qRT-PCR	qRT-PCR	No. Animals for GAPDH assay	qRT-PCR	ISH	qRT-PCR
P1	–	3				–	4
P3	–	4		6		–	6
P4	6	–				6	–
P5	5	4	3	7	3	5	3
P6	5	–				5	–
P8	6	5	3			6	4
P12	–	3	3			–	3
P14	6	–				5	–
TOTAL	28	19	9	13	3	27	20

amplification was as follows: 1 cycle at 95°C for 5 min; 30 cycles of 94°C for 1 min, 65°C for 1 min, and 75°C for 2 min. Ephrin-A5 PCR amplification was as follows: 1 cycle at 95°C for 2 min, 35 cycles at 94°C for 1 min, 62°C for 1 min, and 72°C for 1 min; followed by 1 cycle at 70°C for 10 min. The expected bands were isolated from agarose and polyacrylamide gels, then DNA was extracted and subcloned into pCRII® vector (TA cloning kit, Invitrogen, Carlsbad, CA) and sequenced (at the BioResource Center, Cornell University, or in the DNA/Protein Core Facility at Georgia State University). Sequence analysis was carried out using Lasergene (DNAStar, Madison, WI) and Sequencher software (Genecodes, Ann Arbor, MI).

In Situ Hybridization

The aforementioned ephrin-A5 clones served as templates for the production of riboprobes for *in situ* hybridization. Plasmids containing the PCR fragments were linearized with the restriction enzymes *Hind III* and *Xba* I followed by *in vitro* transcription with T7 and Sp6 to synthesize [^{35}S]-CTP (New England Nuclear, Boston, MA)-labeled antisense and sense riboprobes. Sections were fixed in 4% paraformaldehyde in 0.1 *M* Phosphate Buffered Saline (PBS) (pH 7.4), rinsed twice in 0.1 *M* PBS, then treated with proteinase K (10 μg/mL) diluted in TE (50 m*M* Tris-HCl pH 8.0 and 5 m*M* EDTA) for 10 min while stirring. Sections were acetylated and then dehydrated in 70%, 95%, and 100% ethanol (3 min each). To delipidize the tissues, sections were washed in 100% chloroform, 100% ethanol, and 95% ethanol, followed by prehybridization in a 50°C oven for 2 h. For the hybridization, [^{35}S]-riboprobes were fragmented to improve penetration and applied to the sections overnight at 50°C. Sections were then washed under stringent conditions and treated with RNaseA at 37°C for 30 min. Lastly, sections were dehydrated, air dried, and placed on Kodak film (BioMax MR, Eastman Kodak Co.) with ^{14}C microscales (Amersham Pharmacia Biotech, Piscataway, NJ) for 2 to 3 weeks. The film was then developed and dried (Model SRX-101A film processor, Konica Corporation, Tokyo, Japan). Sense riboprobe controls were included in each case to ensure the specificity of the radiolabel. Radiolabel above background levels was not observed on control sections incubated with sense riboprobe.

Quantitative Real-Time PCR

The standardized qRT-PCR procedure provides an absolute measurement of gene expression in units of mRNA copy number per quantity of total cDNA. This measure is thus independent of the amount of tissue analyzed. This was particularly important for this analysis because SC size varied by age and treatment group. In order to assay how ephrin-A2 and ephrin-A5 expression changes from anterior to posterior in SC, each right superior colliculus from normal and PT hamsters at postnatal ages P1, 3, 5, 8, and 12 was divided into thirds along the anteroposterior axis. The anterior third and posterior third were analyzed in parallel and the middle third was discarded. In a control group of animals, we divided the anterior half of the normal SC into thirds and repeated the procedure at P5, P8, and P12. This half-normal group was included to control for SC position as a determinant of ephrin expression level, given that in the PT lesioned animals approximately the posterior half of SC is removed. This ensures that the position of the anterior and posterior thirds of the Half-Normal and PT SCs are roughly equivalent. Sham surgery animals were included at age P5 only. Three animals were used for each of four groups—Normal, Half-Normal, Sham, and PT. All dissections were done under RNAse-free conditions.

For preparing tissue for analysis, total RNA from each sample was isolated using a PicoPure™ RNA isolation Kit (Arcturus Bioscience Inc., Mountain View, CA) according to manufacturer directions. RNA was treated with DNase I (Qiagen Inc., Valencia, CA) to remove any genomic DNA. RNA quality was assessed with an Agilent 2100 bioanalyzer (Agilent Technologies, Palo Alto, CA). Reverse transcription was performed using SuperScript II™ Reverse Transcriptase (Invitrogen Corp, Carlsbad, CA), according to the manufacturer's protocol. The concentrations of the resulting cDNAs were measured in triplicate with a BioPhotometer (Brinkmann Instruments Inc., Westbury, NY). An ABI PRISM 7700 Detection System (Applied BioSystems, Foster City, CA) was used. TaqMan™ PCR forward

and reverse primers and target-specific fluorogenic probes were designed based on hamster sequences, using ABI Primer Expression software (Applied BioSystems, Foster City, CA). Each PCR reaction consisted of 200 ng cDNA, 800 n*M* forward and reverse primers, 100 n*M* hybridization probe, and Taqman™ Master Mix, for a final volume of 30 μL. Primers and probes used were as follows: ephrin-A2: forward primer: 5'-TGGAGCGGTACATCCTGTACAT-3'. Reverse primer: 5'-TGCATTCCCAGCGCTTG-3'. Probe: 5'-FAM CATGCGTCCTGCGACCACCG TAMRA-3'. Ephrin-A5: forward primer 5'-TGTCCTCTACATGGTGA ACTTTGAC-3'. Reverse primer 5'-GCCGGTTACATTCC CATCTCT-3'. Probe 5'-FAM CCTGCGACCACACTTC CAAAGGCT TAMRA-3'.

PCRs were run in triplicate at 50°C for 2 min and 95°C for 10 min, followed by 40 cycles at 95°C for 15 sec and at 60°C for 1 min. Standard curves were generated by three independent serial 1:10 dilutions of cloned plasmid DNA for each of the genes, run in duplicate. The dilutions were made over a range that considered the expected amount in the samples. The PCR products were confirmed by gel electrophoresis. In addition, a conventional PCR omitting the hybridization probe was run in parallel on a thermocycler to verify PCR specificity.

Several controls were included to test the specificity of the results. Expression levels of ephrin-A5 and -A2 in normal and lesioned SC were compared with those taken from the unlesioned side of SC and from the cerebellum. For these assays we measured relative mRNA copy number in reference to the housekeeping gene GAPDH in three animals from each group. We chose GAPDH because its expression remained stable in a previous study of traumatic brain injury (Cook et al., 2009). Total RNA was isolated (100 ng/sample, RNeasy Isolation Kit, Qiagen Inc., Valencia, CA), and cDNA was synthesized from total RNA as described above. Concentrations of total RNA and cDNA were measured in triplicate (BioPhotometer, Eppendorf Instruments Inc., Westbury, NY). Probes and primers for ephrin-A5 and -A2 were as described above, and GAPDH probes and primers were obtained from TaqMan Gene Expression Assays (Applied BioSystems, Foster City, CA). An ABI PRISM 7700 Fast Real Time PCR System was used for qRT-PCR using the comparative C_T method (2-(DeltaDeltaC(T)) method) (Applied BioSystems, Foster City, CA) (Schmittgen and Livak, 2008). PCR reactions were run in triplicate at 95°C for 20 s and 60°C for 30 s, followed by 40 cycles at 95°C for 30 s. The cycle threshold (Ct) was used to compare expression of the gene of interest across the different experimental groups. To verify PCR specificity, a negative control omitting hybridization probes was run in triplicate.

Data Analysis

To estimate ephrin mRNA distribution along the anteroposterior axis of the SC, digital images of three adjacent parasagittal sections were captured from the *in situ* hybridization films using a MCID workstation (Version 6.0, Imaging Research Inc. Ontario, Canada). Images were imported into NIH Image (ver. 1.62) and standardized using the ^{14}C microscales that had been placed in the film cassette along with the ^{35}S labeled parasagittal sections. After subtracting the off-section background label from the optical density values for each section, the freehand drawing segment tool was used to trace along the anteroposterior axis of the superficial gray layer of the SC. The level of ephrin expression at each location along this anteroposterior tracing was obtained for each of the three sections using the plot profile option, and the data were transported into a Microsoft Excel spreadsheet. To acquire relative optical density values for anterior, middle, and posterior portions of SC, the density measurements taken along the anteroposterior axis were divided into equal anterior, middle, and posterior thirds, and an average optical density calculated for each third independently. In this way we could compare across colliculi of different lengths (SC length increases with age and is decreased in lesioned colliculi). The resulting three average OD values were then plotted against the measured distance along the anteroposterior length of the SC, and the slope of the density gradient (Δ O.D./Δ mm) was determined by linear regression for each section using commercial statistical software (SigmaPlot, Systat Software Inc., Richmond, CA). Note that in the lesioned animals the posterior limit of the SC is reached in a shorter distance than in normal animals. For each animal, the slopes of the ephrin expression gradients for the three sections from each animal were averaged, and the means of these averages were then calculated from each experimental group (Normal or PT) at each postnatal age. Our hypothesis predicts that if the ephrin gradient compresses, the Δ O.D./Δ mm value would double with a 50% lesion. Alternatively, if the ephrin gradient is not affected by the PT map compression, then the Δ O.D./Δ mm value would remain the same as in normals. For statistical comparisons, we used either *t*-tests or a two-way ANOVA followed by a Tukey *post hoc* test for the pairwise comparisons (SigmaStat, Systat Software Inc., Richmond, CA) to measure the variability between animals and within and between treatment groups and age.

RESULTS

This study examined the relationship between retinocollicular map compression and the expression gradients of the ephrin-A2 and -A5 ligands for Eph tyrosine kinase receptors (Fig. 1). To determine whether a redistribution of ephrin-A2 and/or A5 mRNA is associated with partial (PT) SC ablation, we analyzed the expression of the genes using both quantitative real-time PCR and *in situ* hybridization (ISH).

Animals

The number and postnatal ages of the animals (Syrian hamsters) used in this study are indicated in Table 1.

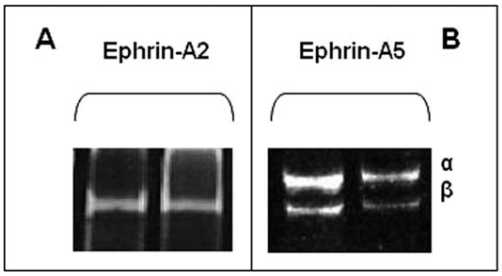

Figure 2 Cloning of ephrin-A2 and ephrin-A5. Partial sequences of the two ephrins were obtained using a degenerate PCR strategy. A. One clone was obtained for ephrin-A2 at 346 base pairs (bp). B. For ephrin-A5 two isoforms were cloned, A5α (625 bp) and A5β (544 bp). Each gel shows duplicate samples.

In total, 59 normal animals were used for ephrin assays (including three for sham surgeries and nine for Half-Normal-sized SC controls) and 3 for GAPDH assays. Forty-seven PT animals were used for ephrin assays and 4 for GAPDH assays. Their ages ranged from postnatal day (P)1 to P14, with the day of birth designated as P0. At least three and at most six animals at each age and condition were included.

Cloning Hamster Orthologs of Ephrin-A2 and -A5

We produced partial clones of the homologous hamster ephrin-A2 and -A5 orthologs using a degenerate primer strategy based on conserved regions of human and mouse ephrin-A genes (GenBank accession numbers for ephrin-A2: DQ630462; ephrin-A5α: DQ630463; ephrin-A5β: DQ630464; see Methods). The ephrin-A2 clone was 346 base pairs (bp) in length. Two isoforms of ephrin-A5 were cloned, A5α (625 bp) and A5β (544 bp) (Fig. 2). Interestingly, ephrin-A5β lacks an alternatively spliced 27 amino acid exon found in ephrin-A5α. This exon is also known to be alternatively spliced in mice (Flenniken et al., 1996) and in rats (Lai et al., 1999). Thus, alternative splicing of ephrin-A5 is highly conserved across rodent species, suggesting distinct functions for each isoform. Predicted Syrian hamster ephrin-A2, ephrin-A5α, and ephrin-A5β proteins were aligned with known mouse and human sequences (Table 2). The cloned fragment of hamster ephrin-A2 was 95% identical to mouse and 92.1% identical to human sequences. Hamster ephrin-A5α was 100% identical to mouse and 99.6% identical to human ephrin-A5. Hamster ephrin-A5β was 99.1% identical to mouse and 98.7% identical to human sequences (not shown; see Genbank accession numbers ephrin-A2: mouse NP_031935; human NP_001396; ephrin-A5: mouse AAB50240; human NP_001953). Once cloned, the partial sequences were then used to design specific hybridization probes and primers for ISH and QRT-PCR.

Normal Animals

The Spatiotemporal Gradient of Ephrin Expression in Hamsters Resembles that Seen in Other Species. Because the goal of this study was to uncover general principles regarding the role of ephrin-As in mammalian brain development, we first sought to establish whether the spatiotemporal pattern of expression in Syrian hamsters is similar to that in mice, which are more typically used in mammalian gene expression assays. Hamsters are born at an earlier stage of development than mice (Clancy et al., 2001), thus we had the advantage of a longer period of postnatal ephrin expression in this rodent species. The immature state of the brain at birth makes Syrian hamsters an ideal model for developmental studies.

Quantitative real-time PCR was used to measure absolute mRNA copy number in reference to a standard curve. In normal hamster pups aged from P1 to P12, the superficial SC was trisected along its length, and tissue from the anterior and posterior thirds was extracted and homogenized for PCR. During this developmental time period, the retina is forming synaptic connections with the SC but the eyes have not opened. The same tissue was used for both ephrin-A2 and ephrin-A5 measurements at each age. We did not attempt to distinguish between ephrin-A5α and ephrin-A5β, because the probes we used could potentially bind to either isoform.

Our qRT-PCR data from normal animals revealed that ephrin-A2 and -A5 expression in SC was sharply graded in a low anterior to high posterior direction, and that expression declined with age (Fig. 3). This pattern was consistent with that seen in other species, including mice (see Drescher et al., 1997; O'Leary and McLaughlin, 2004, for review). In the normal animals, expression was higher overall in posterior than in anterior SC (two-way ANOVA, $p < 0.02$). This difference was especially prominent at the earlier ages. Pair-wise comparisons at each age revealed significant anteroposterior differences at P1-P5 for ephrin-A5 [Fig. 3(A)] and at P1-P3 for ephrin-A2 [Fig. 3(B)] ($p < 0.01$ for ephrin-A5 and $p < 0.001$ for ephrin-A2; Tukey test for *post hoc* pair-wise comparisons). Ephrin-A5 expression was highest at P1 and P3, but levels were intermediate at P5. By P8 the

Table 2 Nucleotide and Translated Amino Acid Sequences for the Three Partial Ephrin-A Clones used in this Study

ephrin-A5 nucleotide and amino acid sequence[a]	atgttgacgctgctctttctggtgctctggatgtgtgtgttcagccaggacccgggctcc atgttgacgctgctctttctggtgctctggatgtgtgtgttcagccaggacccgggctcc M L T L L F L V L W M C V F S Q D P G S ggtgattaccacatagacgtctgtatcaatgactacctggacgttttctgccctcactat ggtgattaccacatagacgtctgtatcaatgactacctggacgttttctgccctcactat G D Y H I D V C I N D Y L D V F C P H Y gaggactctgtcccagaagataagactgaacgctatgtcctctacatggtgaactttgac gaggactctgtcccagaagataagactgaacgctatgtcctctacatggtgaactttgac E D S V P E D K T E R Y V L Y M V N F D ggctacagtgcctgcgaccacacttccaaaggcttcaagagatgggaatgtaaccggcct ggctacngtgcctgngaccncacttccaaaggcttcaagagatgggaatgtaaccggcct G Y S A C D H T S K G F K R W E C N R P cactctccaaatggaccgctgaagttctcggaaaaattccagctcttcactccctttcc cactctccaaatggaccgctgaagttctcggaaaaattccagctcttcactccctttcc H S P N G P L K F S E K F Q L F T P F S cttggatttgaattcaggccaggccgagagtatttctacatctcttctgcgatcccagac cttggatttgaattcnggccaggccgagagtatttctacatctcttctgcgatcccagac L G F E F R P G R E Y F Y I S S A I P D aacggaagaaggtcctgcctaaaactcaaagtcttcgtgagaccaacaaatagctgtatg aacggaagaaggtcctgcctaaaactcaaagtcttcgtgagaccaacaaat--------- N G R R S C L K L K V F V R P T N S C M aaaactataggtgttcatgatcgtgttttcgatgttaacgacaaagtagaaaattcatta ---------- K T I G V H D R V F D V N D K V E N S L gaaccagcagatgataccgtacacgagtcagccgagccatcccgcggtgagaacgcggcg ----------gataccgtacacgagtcagccgagctatcccgcggtgagaacgcggcg E P A D D T V H E S A E P S R G E N A A cagacaccaaggatacccagccgc catacaccaaggatacccagncgc Q T P R I P S R
ephrin-A5 protein alignment[a]	----------MLTLLFLVLWMCVFSQDPGSKVVADRYAVYWNSSNPRFQRG **Hamster α** ----------MLTLLFLVLWMCVFSQDPGSKVVADRYAVYWNSSNPRFQRG **Hamster β** MLHVEMLTLLFLVLWMCVFSQDPGSKVVADRYAVYWNSSNPRFQRG **Mouse** MLHVEMLTL**V**FLVLWMCVFSQDPGSK**A**VADRYAVYWNSSNPRFQRG **Human** DYHIDVCINDYLDVFCPHYEDSVPEDKTERYVLYMVNFDGYSACDH DYHIDVCINDYLDVFCPHYEDSVPEDKTERYVLYMVNFDGYSACDH DYHIDVCINDYLDVFCPHYEDSVPEDKTERYVLYMVNFDGYSACDH DYHIDVCINDYLDVFCPHYEDSVPEDKTERYVLYMVNFDGYSACDH TSKGFKRWECNRPHSPNGPLKFSEKFQLFTPFSLGFEFRPGREYFY TSKGFKRWECNRPHSPNGPLKFSEKFQLFTPFSLGFEFRPGREYFY TSKGFKRWECNRPHSPNGPLKFSEKFQLFTPFSLGFEFRPGREYFY TSKGFKRWECNRPHSPNGPLKFSEKFQLFTPFSLGFEFRPGREYFY ISSAIPDNGRRSCLKLKVFVRPTNSCMKTIGVHDRVFDVNDKVENS ISSAIPDNGRRSCLKLKVFVRPTN---------- ISSAIPDNGRRSCLKLKVFVRPTN---------- ISSAIPDNGRRSCLKLKVFVRPTNSCMKTIGVHDRVFDVNDKVENS LEPADDTVHESAEPSRGENAAQTPRIPSR---------- ----------DTVHESAELSRGENAAXTPRIPSR---------- ----------DTVHESAEPSRGENAAQTPRIPSRLLAILLFLLAMLLTL LEPADDTVHESAEPSRGENAAQTPRIPSRLLAILLFLLAMLLTL

Table 2 (***Continued***)

ephrin-A2 nucleotide and amino acid sequence[b]	gcccgggccaacgctgaccgatacgcagtctactggaaccgcagcaaccccaggtttcag A R A N A D R Y A V Y W N R S N P R F Q gtgggcaccctgggagacggtggcggctacacggtggaggtaagcatcaatgactatctg V G T L G D G G G Y T V E V S I N D Y L gacatctactcccgcactacggggccccgctgcccccggccgagcgcatggagcggtaca D I Y C P H Y G A P L P P A E R M E R Y tcctgtacatggtgaacggcgagggtcatgcgtcctgcgaccaccggcaccgaggcttca I L Y M V N G E G H A S C D H R H R G F agcgctgggaatgcaagcggcccgcagcacccgggggggcccctcaagttctcagagaagt K R W E C X R P A A P G G P L K F S E K tccaactcttcacccccttttccctgggctttgagttccggc F Q L F T P F S L G F E F R
ephrin-A2 protein alignment[b]	----------ARANADRYAVYWNRSNPRFQV **Hamster** MAPAQRPLLPLLLLLLPLR------ARNEDPARANADRYAVYWNRSNPRFQV **Mouse** MAPAQAPLLPLLLLLLPLPPPPFARAEDAARANSDRYAVYWNRSNPRFHA **Human** -GTLGDGGGYTVEVSINDYLDIYCPHYGAPLPPAERMERYILYMVNGEGHA -SAVGDGGGYTVEVSINDYLDIYCPHYGAPLPPAERMERYILYMVNGEGHA GAGDDGGGYTVEVSINDYLDIYCPHYGAPLPPAERMEHYVLYMVNGEGHA SCDHRHRGFKRWECXRPAAPGGPLKFSEKF---------- SCDHRQRGFKRWECNRPAAPGGPLKFSEKFQLFTPFSLGFEFRPHGEYYY SCDHRQRGFKRWECNRPAAPGGPLKFSEKFQLFTPFSLGFEFRPHGEYYY

[a]The two ephrin-A5 clones, α and β, were 625 bp and 544 bp in size, respectively.

[b]The ephrin-A2 clone was 346 bp in length. Comparisons with mouse and human clones are shown in register (GenBank accession numbers for ephrin-A5α: DQ630463; ephrin-A5β: DQ630464; ephrin-A2: DQ630462).

level of ephrin-A5 expression was low. Ephrin-A2 expression levels were highest at P1 and P3, and declined markedly by P5. The expression levels of ephrin-A2 were approximately double those of ephrin-A5 overall. Thus the spatiotemporal pattern of ephrin expression in hamster SC appears similar to that reported in fish, chicks and mice (Cheng and Flanagan, 1994; Cheng et al., 1995; Drescher et al., 1997; Picker et al., 1999).

The disadvantage of the qRT-PCR approach is that it requires homogenizing the tissue, preventing detailed visualization of the spatial pattern of mRNA expression. In order to examine the spatial distribution of ephrin-As across the SC, we employed *in situ* hybridization (ISH) in parasagitally-sectioned brains using ^{35}S-labeled riboprobes. Ephrin-A5 and not ephrin-A2 riboprobes were used for ISH, because ephrin-A5 mRNA was more efficiently detected with the probes we designed, and because previous studies in mice have shown that knockout of ephrin-A5 has a greater effect on retinal axon targeting than knockout of ephrin-A2 (Frisén et al., 1998; Feldheim et al., 2000). Furthermore, ephrin-A5 is reportedly expressed in a more steadily increasing gradient than ephrin-A2. The latter attains maximum expression in central SC (Feldheim et al., 2000; Yamada et al., 2001). To obtain a relative quantification of the mRNA signal throughout development, the optical density of radiolabel was measured along the anteroposterior axis of the SC in serial sections using animals of different postnatal ages (see Methods for details).

We observed an anteroposterior gradient of ephrin-A5 expression in normal animals that increased gradually in the anterior half then increased more steeply toward the posterior half of superficial SC, extending into deeper SC layers at the posterior edge (Fig. 4). This overall pattern was present throughout the first 2 postnatal weeks. In agreement with the qRT-PCR results, the ISH data demonstrated that ephrin-A5 expression declined with age. Expression was highest during the first postnatal week. This pattern of ephrin-A5 mRNA expression is similar to that reported in other rodent species and in birds (mouse: (Feldheim et al., 1998); rat: (Symonds et al., 2001); chick:

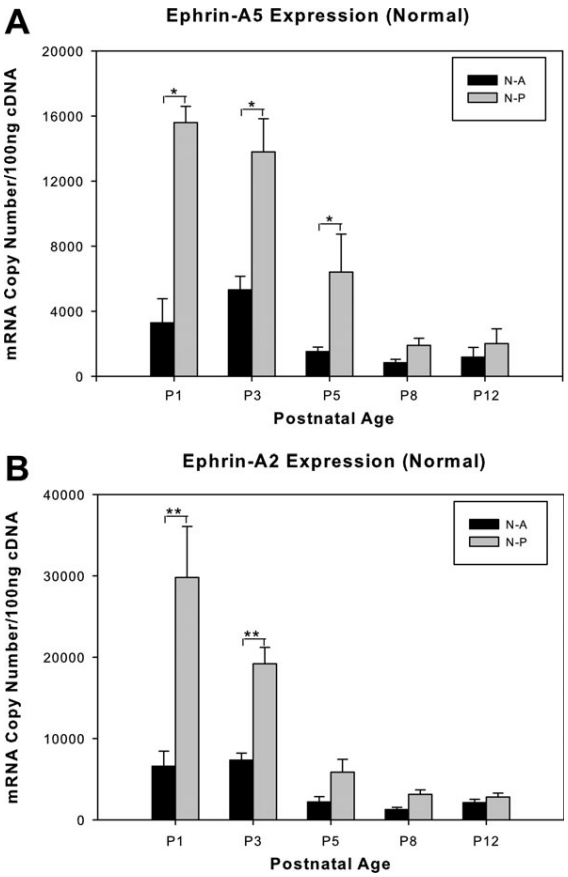

Figure 3 Quantitative real-time PCR analysis of normal hamster ephrin-A5 and ephrin-A2 expression. Quantified (A) ephrin-A5 and (B) ephrin-A2 mRNA levels were lower in anterior than in posterior SC at all postnatal ages assessed (P1, P3, P5, P8, and P12) in normal (N) animals. The overall mRNA levels decreased with age, as did the relative difference between anterior and posterior expression levels. A-anterior, P-posterior. Data presented as mean ± SE, two-way ANOVA with Tukey tests for pairwise comparisons; $*p < 0.01$; $**p < 0.001$.

(Yamada et al., 2001)), and resembles somewhat the protein expression pattern reported for ephrin-A2 in hamsters (Lukehurst et al., 2006). We conclude from the qRT-PCR and ISH data that Syrian hamsters, with their short gestation, protracted postnatal brain development, and demonstrated retinocollicular map plasticity (Finlay et al., 1979; Pallas and Finlay, 1989, 1991), are an ideal model system for investigating developmental plasticity of ephrin function.

Lesioned Animals

The Major Features of the Ephrin Gradient are Maintained in Compressed Maps. Neonatal ablations of less than 70% of the SC reliably lead to retinocollicular map compression (Finlay et al., 1979; Pallas and Finlay, 1989). To test the hypothesis that map compression is associated with a compression of the ephrin gradient, we examined the effect of a partial (PT) ablation of posterior SC on ephrin expression along the anteroposterior axis of hamster SC. A compression of the ephrin guidance cues could direct the compression of the retinal projection, providing a mechanism to explain how the SC recovers from neonatal damage (Finlay et al., 1979; Pallas and Finlay, 1989). We employed the two complementary techniques, quantitative real-time PCR and *in situ* hybridization, in order to reveal both the amount and the spatial distribution of ephrin-A in the partially lesioned SC.

The qRT-PCR measurements revealed that the anteroposterior gradient in ephrin expression was also present in the compressed maps of PT-lesioned animals by 5 days post-lesion (Fig. 5). Data obtained from lesioned animals at P5, 8, and 12 showed that expression was significantly higher in posterior than in anterior SC for both ephrin-A5 [$p < 0.05$, two-way ANOVA; Fig. 5(A)] and ephrin-A2 [$p < 0.02$, two-way ANOVA; Fig. 5(B)]. Pairwise comparisons (Tukey test) revealed a significant difference between treatment groups in expression at P5 ($p < 0.02$) for both ephrin-A5 and ephrin-A2. As in normal animals, the gradient and the expression of these ephrin-As in SC of the PT group begins to decrease with age (cf. Fig. 3). Variability in expression levels was higher in PT cases than in normal cases, due at least in part to the fact that lesion size varies somewhat between animals (see below).

The Amount of Ephrin Expression is Reduced in Lesioned Animals. Although the general features of the ephrin gradient were unaffected by the loss of target, the *in situ* hybridization results suggested that the quantity of ephrin-A5 mRNA was reduced in the PT animals (Fig. 6). In the P5 and P8 cases examined there appeared to be an overall reduction in the intensity of label in SC (at the same image settings), and there was a reduction in label to a lesser extent in adjacent brain regions. This was quantified in SC using the qRT-PCR method. Quantitative comparison of the expression levels confirmed a marked decline of ephrin-A expression in PT cases compared to Normal cases. This can be seen by examining the y-axes in Figures 3 and 5 in parallel, but for ease of comparison we have replotted the qRT-PCR data for ephrin-A5 and ephrin-A2 from normal and PT cases together (Figs. 7 and 8). We found that the mean levels of ephrin-A5 and -A2 expression in the anterior SC of the PT cases were significantly lower within a few days

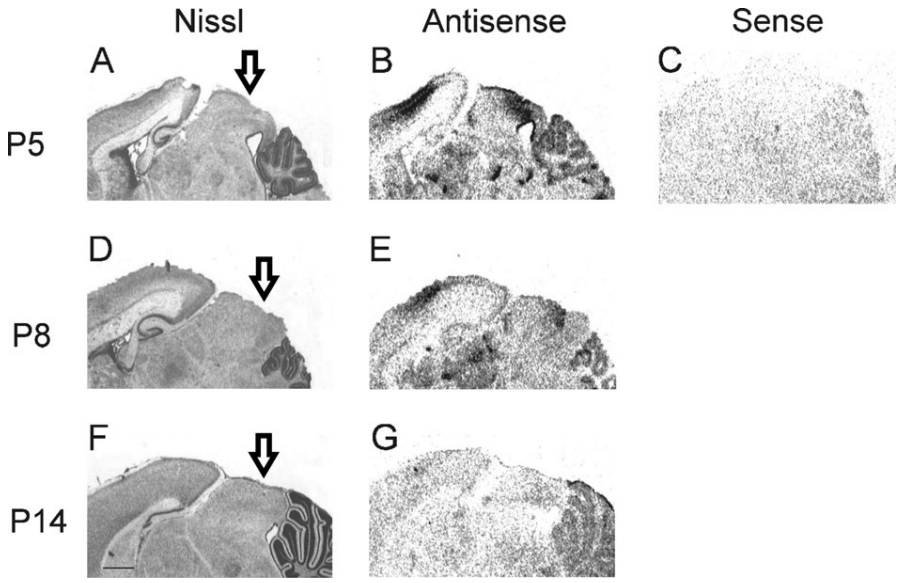

Figure 4 In normal hamster SC ephrin-A mRNA is expressed in an anteroposteriorly increasing gradient that declines with age. A. Nissl-stained, 20 μm parasagittal section from a P5 hamster (anterior is to the left; arrows show the posterior limit of SC). B. Ephrin-A5 ISH expression at P5 revealed with antisense ^{35}S-riboprobes. C. Control section incubated with a sense ^{35}S-riboprobe, showing lack of specific label. D–G. Comparable sections shown at ages P8 and P14. Low anterior to high posterior gradients of ephrin-A5 in SC were maintained throughout the first 2 weeks after birth. The intensity of radiolabeling corresponding to ephrin-A5 decreased as postnatal development proceeded (the 1 mm scale bar in F applies to all panels).

after the lesion (P5 to P12) than those in anterior SC of normal cases ($p < 0.01$, two-way ANOVA; Tukey test for *post hoc* pairwise comparisons, $p < 0.05$ at P5 and P12) [Figs. 7(B) and 8(B), dark bars]. The declines were also seen in posterior SC ($p < 0.02$, two-way ANOVA; Tukey test for *post hoc* pairwise comparisons, $p < 0.01$ at P5) [Figs. 7(B) and 8(B), light bars]. Thus the PT lesions were correlated with overall reductions in expression of ephrin-A5 within a few days after the lesions were performed, although a maximum in the expression gradient was still seen at P5 as in Normal cases. It is important to note that although this decline is intriguing, it is well-documented that relative and not absolute levels of ephrinA expression are the important factor in axon guidance (Brown et al., 2000; Reber et al., 2004; Von Philipsborn et al., 2006).

There are several possible causes for the unexpected but interesting finding that ephrin-A5 expression was reduced in SC of animals with compressed retinocollicular maps. Some reduction in mRNA levels in the posterior third of PT SC was expected to occur, simply because when the posteriorly lesioned SC in PT group cases was divided in thirds for analysis, its posterior third was located in what would have been a more central SC position in an unlesioned animal (see Fig. 1). If this positional difference accounted for the drop in expression, then ephrin expression levels in the anterior third of SC in PTs would be lower than levels in the anterior third of SC in Normals. To test this prediction, we ran quantitative RT-PCR on portions of SC from Normal and PT animals that were similar in position and extent (Half-Normal size SC control group; see Methods) [Fig. 7(C,D)]. We found, as expected, that the position of the tissue sample along the anteroposterior body axis was an important factor in determining the ephrin-A5 expression levels independent of lesion status. When the anterior half of the normal SC was divided in thirds and analyzed to simulate the analysis of the PT lesioned SC, ephrin mRNA expression in the first and last third was lower in the Half-Normal SC group than in the Normal SC group. However, this positional effect did not fully explain the drop in ephrin expression associated with map compression, because the expression in the Half-Normal group, although lower than Normal, was higher than in the PT group. The difference was consistent across ages, and ephrin-A5 expression levels were significantly lower in the PT SC than in the Half-Normal SC in both anterior and posterior samples, at each age ($p < 0.01$ for anterior SC, $p < 0.05$ for posterior SC,

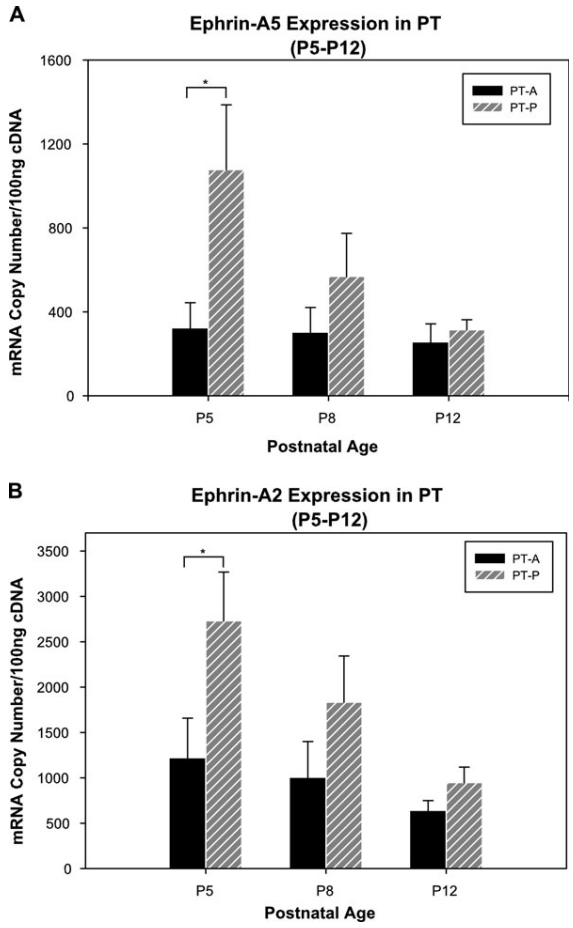

Figure 5 Expression of ephrin-A5 and ephrin-A2 in PT animals is greater in posterior than anterior SC and declines with age. When examined a few days after the posterior SC ablation on P1, the PT cases show a spatial and temporal pattern of expression similar to that seen in normal cases. At P5, P8 and P12, (A) ephrin-A5 and (B) ephrin-A2 mRNA levels were low in anterior SC and high in posterior SC, as in normal animals, and expression levels declined with age. A-anterior, P-posterior, PT-animals with partial SC ablation. Data presented as mean ± SE, two-way ANOVA with Tukey tests for pairwise comparisons; $*p < 0.05$.

two-way ANOVA; Tukey test for *post hoc* pairwise comparisons $p < 0.05$ for P5 and P12 in anterior SC, P5 in posterior SC). Thus, SC tissue sample position did account for some but not the entire decline in expression of ephrin-A5 in PT compared with Normal animals (Table 3).

A similar result was obtained from the qRT-PCR measurements of ephrin-A2 in tissue samples from Half-Normal compared with Normal and PT SC samples. Again the positional effect accounted for some of the differences in expression, and was significant throughout development at the $p < 0.05$ level for anterior SC (two-way ANOVA) but not for posterior SC ($p > 0.1$, two-way ANOVA; pair wise comparisons $p > 0.05$ at all ages in both anterior and posterior SC) (Fig. 8, Table 3). Thus, the reduced ephrin-A expression levels in the SC of PT animals compared with full-size Normal SC can be partially explained by the more anterior location of tissue taken from the PT animals, but the decline in expression associated with the map compression was well beyond what could be accounted for in this way, especially for ephrin-A5. These results suggest that the lesion itself has the effect of reducing ephrin-A expression.

An alternative explanation for the reduced ephrin-A expression in PT cases is that the handling or anesthesia during surgery affects ephrin-A levels. As a control for the effects of the surgical procedures themselves, we performed sham surgeries on some animals at P5 (see Methods). Mean ephrin-A2 and -A5 expression levels at P5 in sham-operated animals were not significantly different from expression levels in normal SC [Normal P5 ($n = 4$) *vs*. Sham P5 ($n = 3$); ephrin-A2 in anterior SC $p > 0.1$ (Student's *t*-test $t = -1.776$); ephrin-A2 in Posterior SC p>0.25 (Student's *t*-test $t = -1.240$); ephrin-A5 in Anterior SC $p > 0.1$ (Mann-Whitney Rank Sum test, $U = 17.0$); ephrin-A5 in posterior SC $p > 0.4$ (Student's *t*-test $t = -0.909$)]. These results show that the reduced expression was unlikely to result from handling stress or anesthesia.

It is possible that neonatal injury to SC results in a nonspecific and general down-regulation of gene

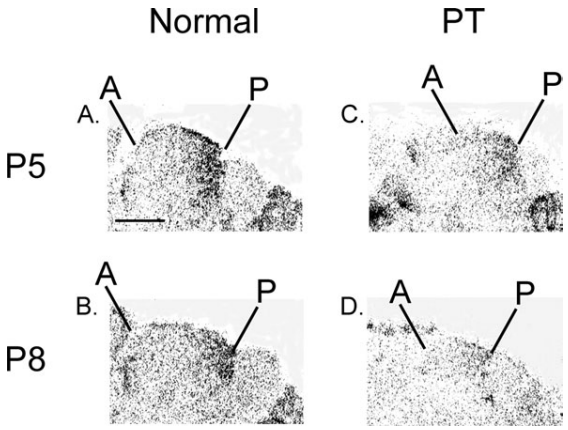

Figure 6 Ephrin-A5 label is reduced in compressed SC. Expression of ephrin-A5 as shown by ISH appeared to be reduced in SC following perinatal damage to posterior tissue (A, P indicate anterior and posterior limits of SC, respectively), but an anterior-posteriorly increasing gradient was still observed. Normal SC at P5 and P8 (A and B) showed a higher intensity of label than PT SC (C and D). Note for each sagittal section: Left = anterior; right = posterior. Scale bar = 1 mm applies to all panels.

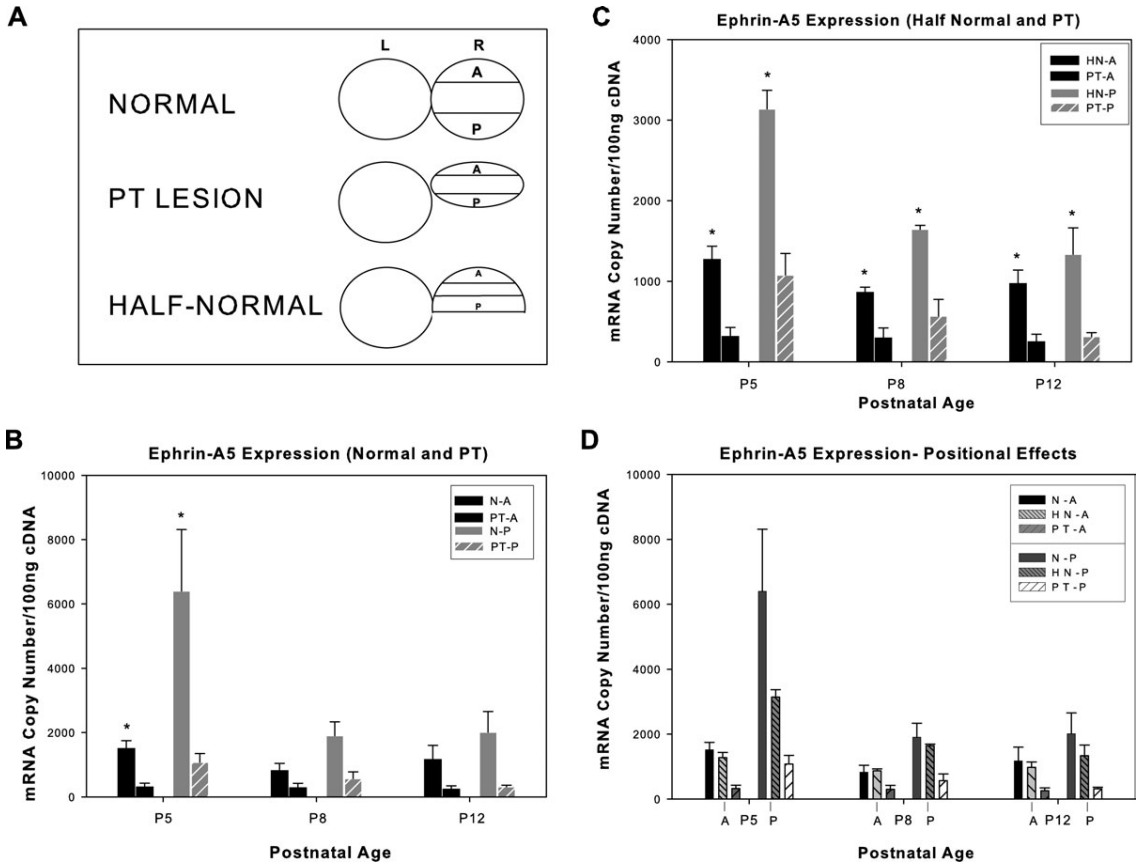

Figure 7 Levels of ephrin-A5 mRNA decrease significantly in PT SC independent of position. Quantitative real-time PCR confirmed the reduced ephrin-A5 expression after injury shown in Figure 6. (A) Expression of ephrin-A5 mRNA in anterior and posterior SC from P5 to P12 was lower in PT than in normal (N) animals. (B) This was true even when SC tissue from comparable anteroposterior levels in normal SC ("Half-Normal", HN) and PT SC was analyzed with respect to ephrin-A5 expression levels. (C) In this plot, the three treatments are presented together for comparison. It can be seen that ephrin-A5 expression in the Half-Normal cases was intermediate between Normal and PT expression levels. See Table 3 for statistical comparisons. Abbreviations as in Figure 5.

expression in the brain, rather than a specific change in ephrin-As. We tested this by measuring levels of the housekeeping gene GAPDH in right SC and in cerebellum (CB) of normal and PT animals. Whereas ephrin-A5 expression in this analysis was significantly reduced in the right SC (RSC) of PT as compared with Normal cases (ephrin-A5 in Normal RSC normalized to 1.00, $n = 3$; mean ephrin-A5 in PT RSC $= 0.24 \pm 0.06$ SEM, $n = 4$; $p < 0.001$, one-way ANOVA using Holms-Sidak method of pairwise comparisons), expression of GAPDH in RSC was not significantly affected by the lesion (GAPDH in Normal RSC normalized to 1.00, $n = 3$; mean GAPDH in PT RSC $= 0.72 \pm 0.02$, $n = 3$; $p > 0.1$, one-way ANOVA using Holms-Sidak method of pairwise comparisons) (Fig. 9), arguing that the effect of the lesion was specific to the ephrin-A5 gene. Neither GAPDH expression nor ephrin-A5 expression in the cerebellum was affected significantly by the lesion in RSC (GAPDH in Normal CB normalized to 1.00, $n = 3$; mean GAPDH in PT CB $= 1.03 \pm 0.13$ SEM, $n = 3$; $p > 0.1$, one-way ANOVA, Holms-Sidak method of pairwise comparisons. Ephrin-A5 in Normal CB normalized to 1.00, $n = 3$; mean ephrin-A5 in PT CB $= 0.78 \pm 0.16$ SEM, $n = 3$; $p > 0.1$, one-way ANOVA, Holms-Sidak method of pairwise comparisons), arguing that the effect was specific to location. These results argue against the possibility that injury causes a global down-regulation of ephrin-A expression.

Another possible explanation for the drop in ephrin-A expression is that tissue damage affects ephrin-A levels at the site of injury alone. Examination of

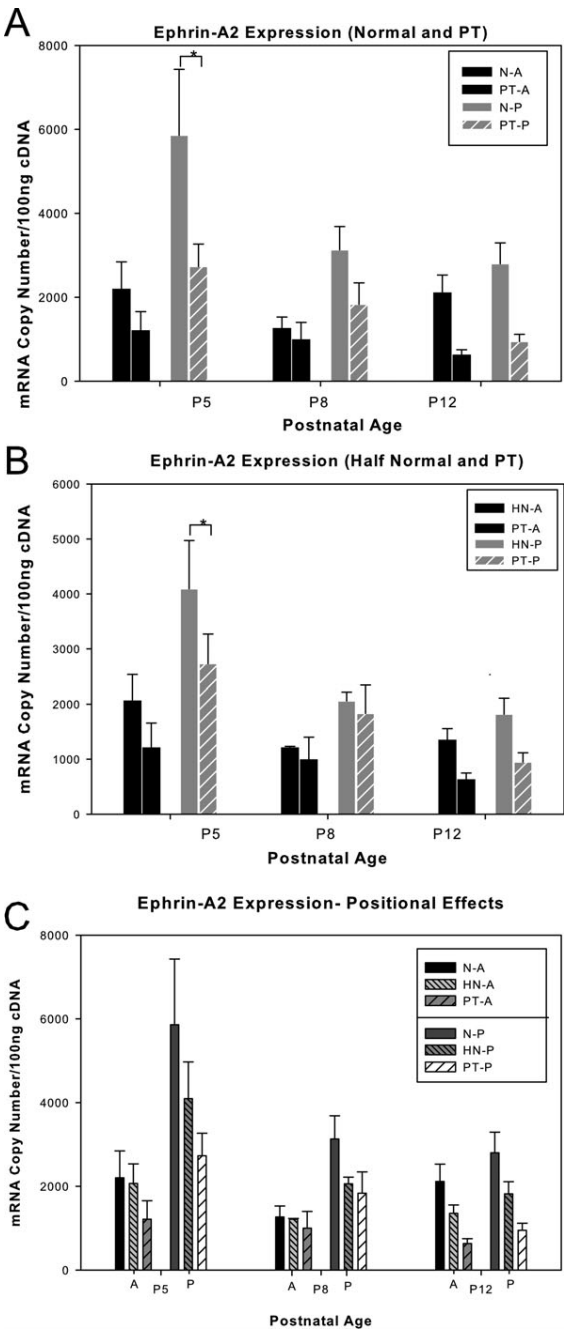

Figure 8 Levels of ephrin-A2 mRNA decrease significantly in PT SC independent of position. (A) As for ephrin-A5, ephrin-A2 mRNA expression in anterior (A) and posterior (P) SC from P5 to P12 was lower in PT than in normal (N) animals. (B) This could only partially be accounted for by absolute position with respect to the anteroposterior axis; compare ephrin-A2 expression levels in HN and PT SC. (C) In this plot the three treatments are presented together for comparison. It can be seen that ephrin-A2 expression in the Half-Normal cases was intermediate between Normal and PT expression levels. See Table 3 for statistical comparisons. Abbreviations as in Figure 5.

Table 3 Reduced Ephrin-A Expression Levels in PT Cases are only Partially Explained by Positional Factors

		Full Normal	Half Normal[a]	*PT*
Ephrin-A5 expression				
P5	A	1517 ± 282	1275 ± 160	321 ± 123[b,c]
	P	6401 ± 1911	3139 ± 231	1077 ± 309[b,c]
		($n = 4$)	($n = 3$)	($n = 3$)
P8	A	829 ± 213	868 ± 60	300 ± 121[b,c]
	P	1904 ± 431	1643 ± 49	569 ± 205[b,c]
		($n = 5$)	($n = 3$)	($n = 4$)
P12	A	1173 ± 424	976 ± 163	254 ± 89[b,c]
	P	2011 ± 642	1335 ± 327	314 ± 48[b,c]
		($n = 3$)	($n = 3$)	($n = 3$)
Ephrin-A2 expression				
P5	A	2203 ± 642	2067 ± 469	1122 ± 510
	P	5859 ± 1571	4093 ± 878	2969 ± 619[b]
		($n = 4$)	($n = 3$)	($n = 3$)
P8	A	1268 ± 261	1214 ± 19	998 ± 402
	P	3129 ± 556	2059 ± 160	1833 ± 509
		($n = 5$)	($n = 3$)	($n = 4$)
P12	A	2116 ± 414	1354 ± 200	633 ± 133[b,c]
	P	2800 ± 495	1819 ± 292	947 ± 197
		($n = 4$)	($n = 3$)	($n = 3$)

[a] Rostral half of Normal SC.
[b] Data significantly different from Full Normal.
[c] Data significantly different from Half-Normal.

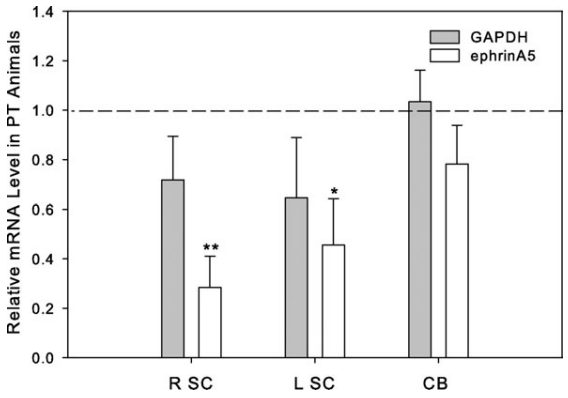

Figure 9 Changes in ephrin-A5 mRNA levels after partial lesion of SC at birth are specific. Relative expression levels of ephrin-A5 or GAPDH mRNA at P5 in ipsilesional (R, right) and contralesional (L, left) SC and cerebellum of PT cases (white bars) were compared with those in normal SC and cerebellum. GAPDH levels were not significantly different from normal in ipsilesional SC of PT animals even though levels of ephrin-A5 in the same tissue were significantly reduced. Expression of both ephrin-A5 and GAPDH was normal in cerebellum of PT animals. In SC contralateral to the lesion ephrin-A5 expression was intermediate between normal and ipsilesional SC but GAPDH expression was unaffected. $*p < 0.05$ and $**p < 0.01$ (one-way ANOVA with Holm-Sidak pairwise comparisons). Error bars indicate mean ± SEM.

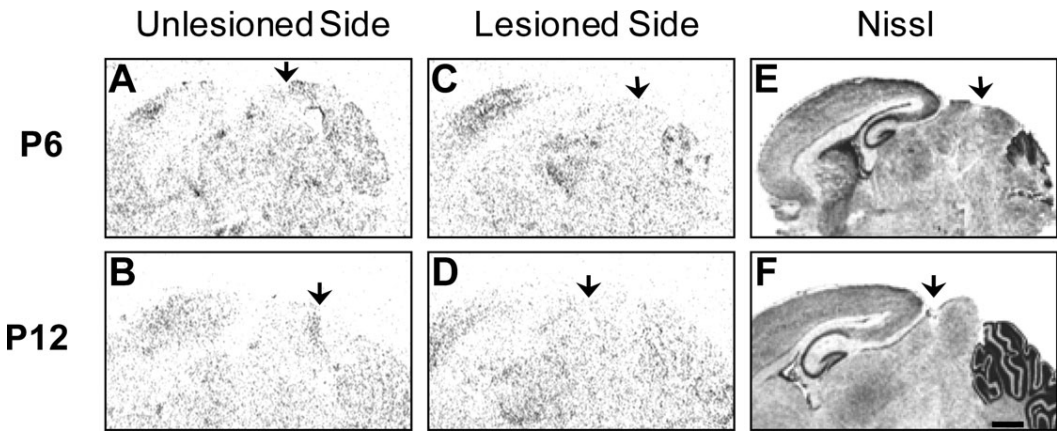

Figure 10 Expression of ephrin-A5 appears reduced in lesioned SC compared with unlesioned SC in the same brain. Sagittal *in situ* hybridization images showing ephrin-A5 expression on the unlesioned side (A, B) and the lesioned side (C–F) of a P6 (A, C, E) and a P12 (B, D, F) hamster suggested that expression of ephrin-A5 was reduced in the lesioned right SC compared with the unlesioned left SC. Scale bar = 1 mm.

ISH sections through the right, lesioned SC compared with those from the left, unlesioned SC at P6 and P12 in two PT animals also demonstrated distance-dependent reductions in ephrin-A expression in SC after damage. The density of ephrin-A5 radiolabel in the unlesioned left SC [Fig. 10(A,B)] appeared higher than that in the lesioned right SC [Fig. 10(C,D)]. To obtain quantitative comparisons, we used qRT-PCR to compare both ephrin-A5 and GAPDH between the lesioned right SC and the unlesioned left SC (Fig. 9). We found that expression of ephrin-A5 in left SC (LSC) contralateral to the lesion was significantly reduced, but to a level intermediate between Normal RSC and PT RSC (ephrin-A5 in Normal LSC normalized to 1.0, $n = 3$; mean ephrin-A5 in LSC of PT = 0.46 ± 0.19 SEM, $n = 3$; $p < 0.05$. Mean ephrin-A5 in PT RSC = 0.28 ± 0.13 SEM, $n = 4$; $p < 0.001$, one-way ANOVA, Holms-Sidak method of pairwise comparisons). At P3, closer to the time of the lesions, the measurements of both ephrin-A5 and ephrin-A2 expression on the unlesioned side of PT cases were intermediate between the expression levels in normal cases and on the lesioned side of PT cases at P3 (Table 4), although the differences were not significant at this age. There was no significant difference between Normal and PT cases in LSC GAPDH expression (GAPDH in Normal LSC normalized to 1.00, $n = 3$; mean GAPDH in PT LSC = 0.65 ± 0.24 SEM, $n = 3$; $p > 0.1$, one-way ANOVA with Holms-Sidak method of pairwise comparisons), indicating the specificity of the effect for ephrin-A5 expression. The intermediate reduction in ephrin-A expression on the unlesioned side of the PT group cases at P5 is consistent with the idea that there is a local effect of the tissue damage on ephrin levels.

Table 4 Effects of Injury on Ephrin Expression are Local

		Normal	Unlesioned Side[a]	*PT*
Ephrin-A5 expression (qRT-PCR)				
P3	A	5,316 ± 827	2,507 ± 979	*1,350* ± 411
	P	13,794 ± 2,035	6,120 ± 3,068	*1,290* ± 592
Ephrin-A2 expression (qRT-PCR)				
P3	A	7,336 ± 871	5,203 ± 1,553	*2,058* ± 507
	P	19,186 ± 2,020	12,174 ± 2,597	3,222 ± 443

[a]There was no significant difference in expression between the unlesioned side of PT cases and that in normal animals at P3. $p > 0.05$, *t*-test.

Taken together, this series of control experiments supports the interpretation that the down-regulation of ephrin-A2 and -A5 expression is both specific to this gene and specific to the site of injury. It is certainly to be expected that early damage to a brain area would cause up or down changes in the expression of many genes, although the methods used here cannot reveal why ephrin-As in particular are down-regulated. Regardless of the cause of the lowered levels of ephrin-As after partial SC ablation, however, they do not prevent the development of a smoothly compressed retinotopic map (Finlay et al., 1979; Pallas and Finlay, 1989; Huang and Pallas, 2001).

The Decline in Ephrin Expression in Lesioned Animals is Initially Delayed in Anterior SC. Another unexpected finding was that the ephrin-A expression gradient in PT animals underwent what at first appeared to be a reversal in the direction of the gradient at P1 to P3. Quantification of ephrin-A mRNA

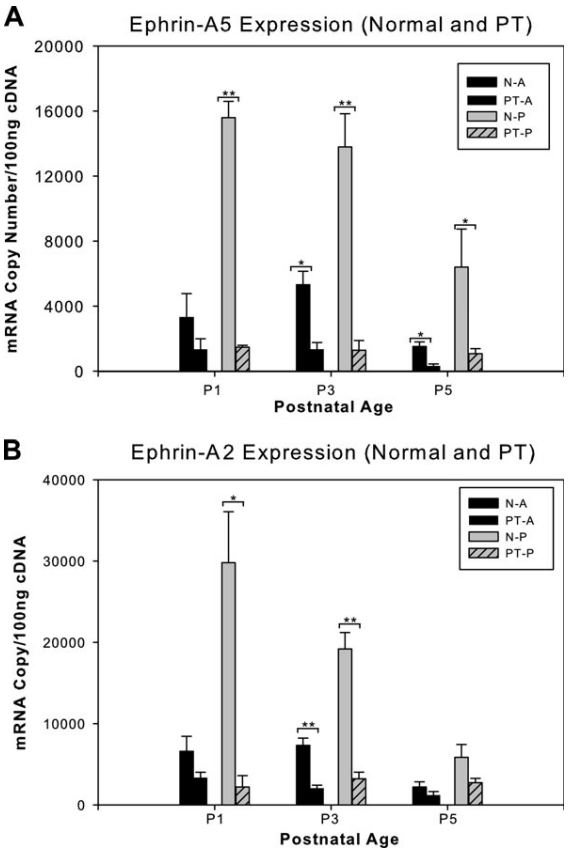

Figure 11 The lesion-induced decline of ephrin expression is delayed immediately after PT lesion. Histograms of (A) ephrin-A5 and (B) ephrin-A2 mRNA levels in normal and PT cases at P1, P3, and P5. One day after the posterior SC is lesioned, the mRNA levels in posterior SC dropped sharply, so that the anteroposterior gradients of ephrin expression were reduced or even reversed at P1. By P5 the gradients had recovered from the lesion and again increased from anterior to posterior. Data presented as mean ± SE, two-way ANOVA with Tukey tests for pairwise comparisons; $*p < 0.05$, $**p < 0.01$.

levels at P1 and P3, after the PT lesion at birth (postnatal day 0), showed that ephrin-A5 and -A2 expression was initially higher in anterior than posterior SC. Looking over a longer time course revealed that, rather than a reversal, there was a delay in the lesion-induced decline of expression in anterior SC compared with posterior SC in the PT animals (Fig. 11). The anteroposteriorly-increasing gradient was re-established by P5 for ephrin-A5 and by P3 for ephrin-A2. This result suggests that the lesion may interrupt an ephrin-A expression-promoting signal from the posterior lesion site that takes several days to reach anterior SC. Another possibility is that the lesion itself directly or indirectly causes a down-regulation of ephrin message that takes time to propagate from posterior to anterior. Although these hypotheses would be interesting to examine further, several studies have shown that relative and not absolute expression levels are important in map formation (e.g. Brown et al., 2000; Reber et al., 2004; von Philipsborn et al., 2006). For this reason, because up or down changes in gene expression levels after brain injury are well-documented, and because our motivation was to investigate the connection between map compression and steepness of ephrin expression gradients, this study did not include further investigations into the reason for the overall drop in ephrin expression level in SC.

The Steepness of the Ephrin-A Gradient Increases in Compressed SC Maps. Of greatest interest in this study was whether the ephrin gradient in animals with compressed maps was altered along the anteroposterior axis in a way that predicts map compression. Because retinal axon targeting is instructed by the concentration gradient of ephrins across the anteroposterior axis of the SC (Frisén et al., 1998), compression of the gradient could be responsible for directing map compression (see Fig. 1). If so, then the ephrin-A gradient in the compressed maps should reach its maximum over a shorter distance; that is, the slope of the gradient should increase in proportion to the post-lesion size of the SC. Using the qRT-PCR data (Table 3) we calculated the posterior to anterior (P/A) ratio of ephrin-A expression to get an initial indication of whether the ephrin-A gradients were steeper in lesioned cases. During the transitional period shortly after the lesion, there was a significant difference in P/A ephrin-A expression ratios between Normal and PT cases (two-way ANOVA, Tukey test for pairwise comparisons, $p < 0.001$ at P1, $p < 0.01$ at P3 for ephrin-A2, $p < 0.01$ at P1 and P3 for ephrin-A5). After the period from P1 to P3, we found that the P/A ratio was approximately the same in the PT cases as in the Normal cases (two-way ANOVA, Tukey test for pairwise comparisons, $p > 0.05$ for both ephrin-A2 and ephrin-A5) (Fig 12). Because the anteroposterior length of SC was shorter in the PT cases, similar P/A ratios indicate a steepening of the gradient. These data are consistent with the hypothesis that the ephrin-A gradient compresses after lesions that lead to compressed retino-SC maps.

The slope of the expression gradient could not be calculated from the homogenized tissue prepared for qRT-PCR, thus we used the ephrin-A5 *in situ* hybridization data to estimate the slope of the concentration gradient (rate of change of ephrin expression with distance across the anteroposterior axis of the SC). The anterior to posterior (rostrocaudal) length of SC was

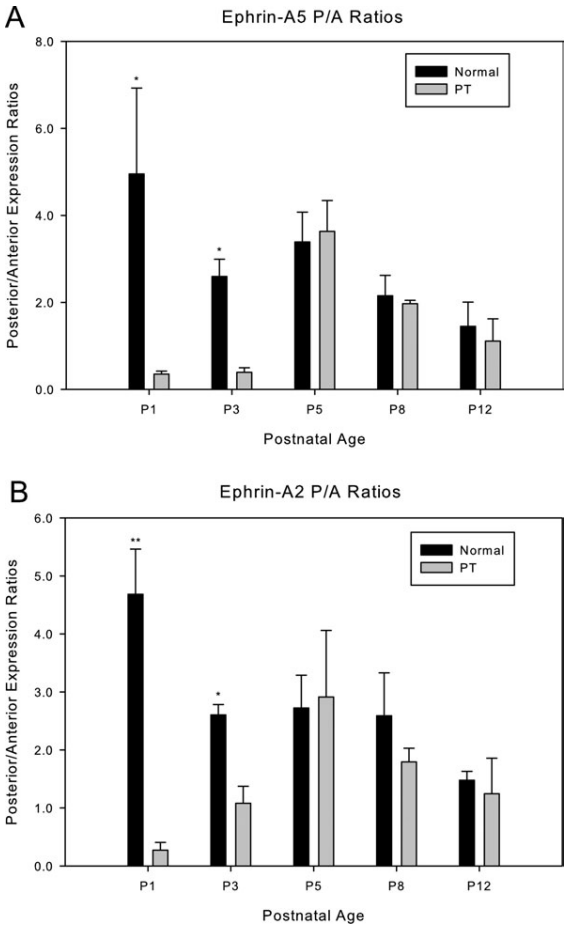

Figure 12 Comparison of anterior versus posterior ephrin-A expression levels. The posterior to anterior ratio of mRNA expression was calculated from quantitative RT-PCR experiments. Because the lesion-induced reduction in expression occurs in posterior SC before that in anterior SC, the P/A ratio indicates anterior levels significantly higher at P1 and P3, comparatively reducing the P/A ratio in the lesioned cases. By P5 the posterior high gradient is restored. Despite the smaller anteroposterior length of SC in the PT cases, there was no significant difference in P/A ratio between Normal and PT cases for either (A) ephrin-A5 ($*p < 0.01$, $**p < 0.001$) or (B) ephrin-A2 ($*p < 0.01$) from P5 and beyond.

measured at comparable mediolateral locations in normal and lesioned cases, and ephrin-A5 expression was quantified using normalized optical density measurements of S^{35} radiolabel along the anteroposterior axis of three adjacent sections from the *in situ* hybridization experiments. We performed this calculation at P5, when the gradient has been re-established. The average optical densities from the anterior, middle, and posterior thirds of SC [Fig. 13(A)] yielded three *y*-axis values of relative ephrin-A5 levels that were used to plot a line against distance on the *x*-axis. The slope of the line (change in ephrin-A5 label with change in distance along the A-P axis) was calculated for each of the three sections and averaged across them. Plotting with this method ensured that the measure of ephrin-A5 gradient slope was independent of the absolute number of ephrin transcripts, and thus provided a measure of gradient steepness independent of the overall reduction in ephrin expression in lesioned animals. As an example, for a 50% lesion, the A-P length of the SC would be 1.0 mm rather than the 2.0 mm typical of normal adult SC. If the ephrin-A5 gradient is compressed into the shortened SC, then the gradient slope should double, supporting the hypothesis, whereas if the gradient is uncompressed the slope would be expected to stay the same [Fig. 13(B)], contrary to the hypothesis.

We found, in support of our hypothesis (see Fig 1), that the slope of the ephrin-A5 gradient was significantly steeper in the PT group compared with the normal group [Fig. 13(C)]; that is, the proportional increase in ephrin-A5 expression per unit distance along the anteroposterior axis of the SC was greater in PT animals than in normal animals. This was true not only at the earlier ages when the normal gradient is steep, but throughout the first 2 weeks of development (two-way ANOVA, $p < 0.001$; Tukey *post hoc* test for pairwise comparisons between normal and PT gave $p < 0.05$ at each age). These data show that the ephrin-A5 expression gradient is compressed in a way that predicts the compression of the retinotopic representation, consistent with a causal relationship between ephrin-A gradient compression and retinocollicular map compression.

DISCUSSION

A number of models have been proposed to explain the processes leading to the development and plasticity of retinotopic maps (Hope et al., 1976; Hope, 1976; Honda, 2004; Koulakov and Tsigankov, 2004; Reber et al., 2004; Lemke and Reber, 2005; Willshaw, 2006; Simpson and Goodhill, 2011; Triplett et al., 2011; Gebhardt et al., 2012). A successful model must be able to incorporate and predict the form of the map under both normal and altered conditions. More recently these alterations have included complex manipulations of gene expression, whereas more classical approaches involved manipulations of afferent/target ratios (Sperry, 1963; Schmidt, 1982; see Udin and Fawcett, 1988, for review). Although genetic approaches have yielded a tremendous amount of information about constraints on possible mapping mechanisms, the mechanism underlying compensation of topographic maps for changes in afferent/target

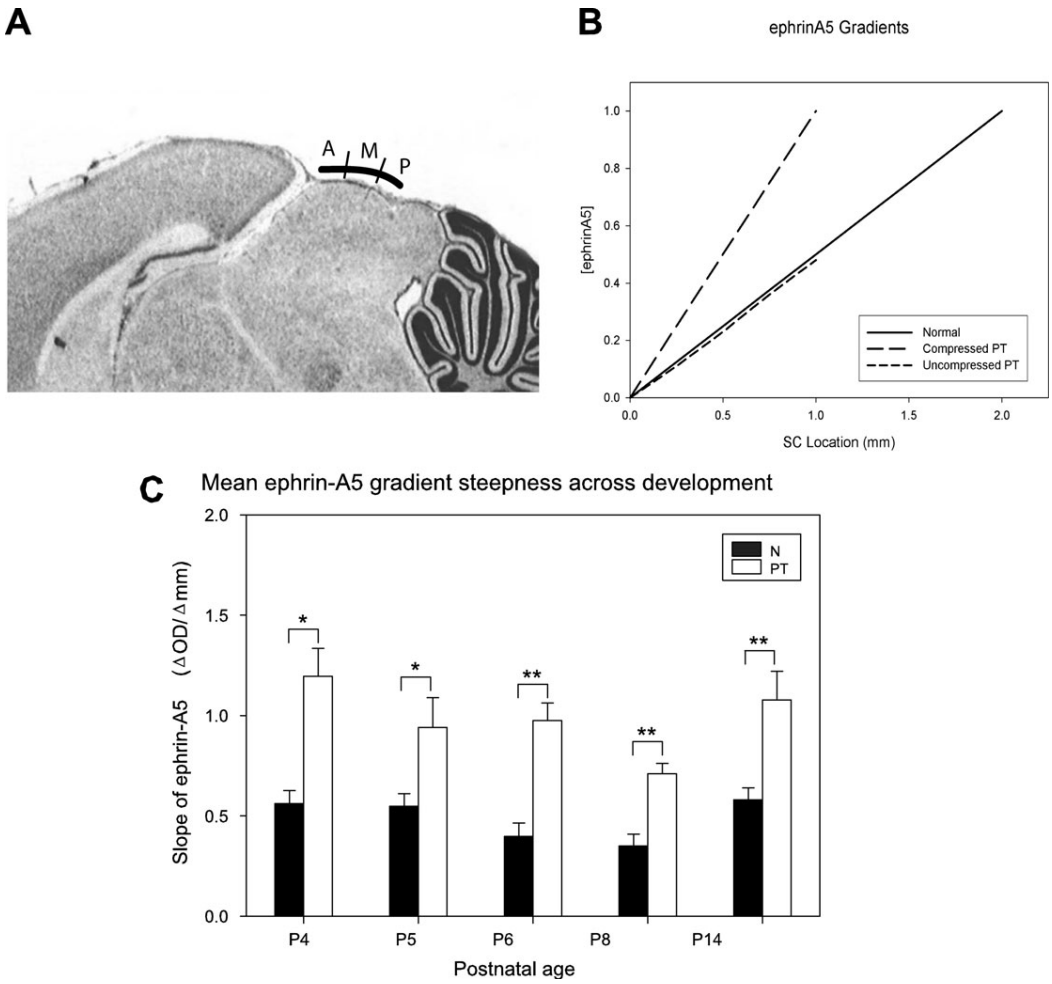

Figure 13 Compression of the ephrin gradient in compressed maps. (A) Optical density measurements taken along the anteroposterior axis of the SC were binned in thirds and averaged to correspond to anterior, middle, and posterior locations in SC, independent of SC length. (B) Cartoon illustrating how these values were then plotted against SC location for calculating the slope of the ephrin gradient. Measurement of expression level as a function of distance along the anteroposterior axis of the SC provided the slope of the ephrin gradient, independent of the lesion size or SC size. Normal SC is approximately 2 mm in anteroposterior length, making an SC with a 50% posterior lesion 1 mm in length. The cartoon illustrates how, according to one hypothesis, the ephrin gradient slope (change in *y*/change in *x*) would get steeper in the smaller SC target, reaching maximum ephrin-A5 levels [ephrin A5] over its extent (Compressed PT gradient). Alternatively, the gradient steepness might be unaffected by the lesion and reach only half the normal maximum at the posterior limit of the lesioned SC (Uncompressed PT gradient). (C) Histogram of mean ephrin-A5 gradient steepness across development taken from QRT-PCR measurements. The slope of the ephrin-A5 gradient was significantly steeper in PT cases compared to normal cases at all ages. Data presented as mean ± SE (two-way ANOVA, $p < 0.001$; Tukey *post hoc* test for pairwise comparisons $p < 0.05$; $^{*}p < 0.05$, $^{**}p < 0.001$).

ratios have never been revealed in the decades post-Sperry. Combining the data generated from these two approaches into one model is an important goal. This study has provided important insight into possible ephrin-A/Eph-A based mechanisms through which topographic maps can be modified after mismatches in afferent/target populations. Our data show that partial ablation of the posterior SC leading to compression of the retinocollicular map is associated with a compression of the ephrin-A gradient. These results suggest that the same molecular mechanisms involved in normal map formation may also be involved in map plas-

ticity, and that they can function adaptively under conditions of increased competition between retinal axons for target space.

Syrian hamsters, a species of altricial, microcricetid rodents (Gattermann et al., 2000), are born early in development and exhibit developmental plasticity in their retinocollicular projection (Finlay et al., 1979), thus they are an excellent model for studying the role of ephrins in map plasticity. Here we provided evidence that Syrian hamsters exhibit similarity in ephrin mRNA sequence and expression with more commonly used animal models such as rats, mice, and chicks. Cloning of ephrin-A2 and ephrin-A5 (Fig. 2) revealed alternate splice forms of ephrin-A5 (A5α and A5β) as seen in mice (Flenniken et al., 1996) and in rats (Lai et al., 1999). The distribution (anterior low, posterior high) and time course of expression (declining with age) of ephrin-A2 and -A5 mRNA in hamsters was similar to that described in other species (Frisén et al., 1998; Wilkinson, 2001) and similar to that described for hamster ephrin-A2 protein (Lukehurst et al., 2006) (Figs. 3 and 4).

Using the clones, we obtained four major results from the PT group of hamsters that underwent neonatal, partial ablation of posterior SC leading to retinocollicular map compression. First, the anteroposteriorly increasing gradient of ephrin-A5 and -A2 expression seen in normal SC maps was re-established in the compressed maps soon after the P0 lesion, by P5 (Fig. 5). Second was the unexpected finding that the number of ephrin-A5 and -A2 transcripts was reduced overall in the lesioned animals compared with normal (Figs. 6) in a way that was specific to position (Figs. 7, 8, and 10) and gene (Fig. 9). Third, this reduction in ephrin-A5 and -A2 expression was delayed in anterior SC compared with posterior SC in the PT animals, resulting in a brief gradient flattening or even reversal in PT animals immediately postlesion (P1-P3) (Fig. 11). Fourth and most importantly for testing our hypothesis, measurements of the steepness of the ephrin gradient in compressed compared with normal maps revealed that the ephrin-A5 gradient compresses along with the map (Figs. 12 and 13), raising the possibility that the compression of the ephrin-A gradient directs map compression. Each of these major findings is considered below.

Gradients of Ephrin-A Gene Expression are Present in Hamster SC under both Normal and Lesioned Conditions

We found that the low anterior to high posterior gradient of ephrin-A2 and -A5 mRNA expression seen in rats and mice (Feldheim et al., 1998; Frisén et al., 1998; Rodger et al., 2001; Symonds et al., 2001) is also present in normal hamsters. Furthermore, as in the other rodent species, expression is highest in the first postnatal week and declines substantially by the end of the second postnatal week. The same is true in the lesioned animals. With the exception of the initial post-lesion recovery period, the expression pattern and time course in lesioned hamsters is very similar to that seen in normal hamsters. These findings suggest that ephrin-A gradients could instruct the formation of the retinotopic map in hamsters as they do in mice (Frisén et al., 1998; Feldheim et al., 2000), and also allow for the possibility that map compression after injury could be guided by the ephrin-As.

Ephrin-A2 and -A5 are Down-Regulated after SC Lesion

We found that the amount of ephrin-A2 and ephrin-A5 mRNA in the developing superior colliculus was substantially reduced as a result of the posterior SC lesions performed at birth. This was an unexpected and interesting finding, given that ephrins are thought to direct map formation and that the retino-SC map forms properly in the lesioned colliculi. It was also unexpected because optic nerve injury in adult rodents resulted in an up-regulation of ephrin-A and a decline in EphA protein expression in SC (Knoll et al., 2001; Rodger et al., 2001, 2005; Symonds et al., 2001, 2007). After brain injury in adult monkeys and humans, EphA receptors are upregulated (Goldshmit and Bourne, 2010; Frugier et al., 2012), and this could lead to changes in ephrin-A ligand levels. Nonetheless, the drop in quantity of ephrin message clearly does not interfere with development of an ordered map, because retinotopically-ordered maps were seen in SC recordings from all treatment groups. Modeling has suggested that neurons can detect small differences in expression of signaling factors of as little as one molecule (Reber et al., 2004; Rosoff et al., 2004). Furthermore, several previous studies have suggested that the quantity of message is not critical (Rosentreter et al., 1998; Brown et al., 2000; Reber et al., 2004; Von Philipsborn et al., 2006) (see below). Reductions in ephrin-A levels could serve a growth-promoting function that may be essential during the recovery process.

We tested alternative hypotheses regarding the cause of the reduction in ephrin-A expression in PT animals: (1) position: the drop could have been because the positional identity of the SC fragments analyzed in PT animals was more anterior than the

equivalent fragments in normal, full-length SC. Analysis of similarly positioned fragments in normal and PT cases provided a partial explanation of the reduction. Even after accounting for position, however, the drop in expression, especially for ephrin-A5, was still substantial. (2) Surgical artifact: the drop could have been due to a general effect of the surgical procedure on ephrin expression in SC. Sham operations had no effect, suggesting that anesthesia and handling stress were not relevant to the experimental outcome. (3) Local damage: the drop could have resulted from a local effect of the early brain damage on adjacent structures. Examination of SC in the hemisphere opposite to the lesion showed ephrin-A5 expression levels midway between normal and PT levels, supporting this hypothesis. Thus the decline in ephrin expression in PT cases can be explained at least in part by both a positional effect and a local damage effect.

There are potential benefits of the decline in ephrin levels if matched by a decline in protein levels. Normally, ephrin clustering occurs in areas of high expression, causing activation of EphA receptors and growth cone collapse. In hamsters with partial ablations of posterior tectum, the number of RGCs remains relatively unchanged (Wikler et al., 1986). Thus in the early stages following the lesion, RGCs containing high levels of EphAs may initially overcrowd anterior SC. A decline in ephrin-As in SC may then allow RGCs expressing high EphAs to arborize within the remaining SC without excess repulsion from high ephrin-A levels. This effect could be facilitated by the growth-promoting effects of low ephrin levels (Hansen et al., 2004). Results from *in vitro* growth cone adaptation assays predict that the retinal axons would adjust to the different levels with time (von Philipsborn et al., 2006), sorting their termination zones according to gradient slope and differences in ephrin-A levels in neighboring neurons rather than absolute levels of ephrin, and allowing ingrowth to continue. It would be interesting to compare the growth rates of nasal and temporal retinal axons as they enter the lesioned SC.

The Lesion-Induced Decline in Ephrin Expression is Delayed in Anterior SC

We found that for 1 to 3 days after the posterior SC ablations, ephrin-A expression levels were higher in anterior than in posterior SC, opposite of normal. The apparent reversal resulted not from an increase in ephrin expression in anterior SC, but from a delay of the lesion-induced decline in expression. The possible explanations of this observation mirror those tested in the context of the overall decline in expression (see above). It may be the case that down-regulation takes longer in anterior SC simply because it is further from the damage. A possible effect of the reversal could be to delay the entrance of nasal retinal axons into the SC for a few days after the lesion. Such a delay could promote recovery from the damage and lead to a more continuously compressed retinocollicular projection. On the other hand, because the levels of ephrin-A are reduced throughout SC in PT cases, ingrowth may be unaffected.

Taken together, the lesion-induced decline in expression and the delay in the propagation of the drop to anterior SC suggest that the lesion interrupts a posterior signaling source that normally maintains ephrin expression at this age. The midbrain/hindbrain boundary (MHB) is a source of signals that affect patterning of the embryonic nervous system (Joyner, 1996), and possible signals that the lesions may affect include FGF8 (Joyner et al., 2000), Otx2/Gbx2 interactions (Li and Joyner, 2001), engrailed (Davis and Joyner, 1988; Friedman and O'Leary, 1996; Logan et al., 1996; Shigetani et al., 1997; Brunet et al., 2005) and Wnt-1 (Dickinson and Mcmahon, 1992, for review; Danielian and Mcmahon, 1996) (Sugiyama et al., 1998). The lesions in this study were made anterior to the MHB on the border between the superior and inferior colliculi (Picker et al., 1999), and thus would not be expected to affect the MHB directly, but could affect propagation of a signal emanating from the MHB. Both en-1 and en-2 are expressed in graded fashion in SC of E17.5 mouse (Davis and Joyner, 1988), which is approximately equivalent in age to a P0 hamster (Clancy et al., 2001), under the direction of MHB signals. Any interruption in en-1/2 could lead to a reduction in ephrin expression. A role for Wnt-1 seems unlikely because Wnt protein secretion reportedly can act only a few cells away (Dickinson et al., 1994). It is not clear whether Wnt-1 protein is expressed in postnatal hamster SC (Wilkinson et al., 1987; Davis and Joyner, 1988; Roelink et al., 1990; Schmitt et al., 2006). These possibilities and other candidate molecules remain to be investigated.

Regardless of the explanation for the reduced levels of ephrin expression in the PT colliculi, our data suggest that the absolute level of ephrin-A mRNA is not critical for map compression as long as the gradient is reestablished. This conclusion is consistent with previous *in vitro* studies in normal animals suggesting that relative and not absolute levels of ephrin and EphA receptors are compared by retinal axons (Rosentreter et al., 1998; Brown et al., 2000) and that axon outgrowth depends on both gradient steepness

and local concentration differences (von Philipsborn et al 2006). Alternatively, it is possible that ephrins are not essential in map compression. This idea is supported by the observation that ephrin-A2/A5 single or double knockouts exhibit only partial mistargeting (Feldheim et al., 2000, 2004). Ephrins may serve simply as one of several polarity cues, with competitive space-filling tendencies explaining the map compression (Constantine-Paton, 1983; Goodhill and Richards, 1999; Feldheim et al., 2000; Ruthazer and Cline, 2004).

Ephrin Gradients are Steeper in Compressed Maps

The main question addressed by our investigation was whether the map compression induced by neonatal partial ablation of posterior SC might be directed by a compression of the ephrin-A2 or -A5 gradient. We showed here that the ephrin-A5 gradient was steeper in compressed retinocollicular maps, but that expression levels were reduced, consistent with the idea that the steepness and relative concentration of the ephrin gradient and not the level of expression are instructive. Levels of EphA receptors or thresholds for promotion or inhibition of axon growth could also be changed in the PT animals, in compensation for the reduced ephrin-A levels. This could occur by ephrin-A concentration-dependent regulation of EphA receptors (Rosentreter et al., 1998; Hornberger et al., 1999). Eph-A and ephrin-A expression are oppositely regulated by FGF *in vitro* (Chen et al., 2009), and thus there is precedent for coordinated regulation of ligand and receptor.

Implications for Developmental and Evolutionary Mechanisms

It is surprising that removal of 50% of a target nucleus in the visual system does not have serious consequences for visual behavior (Finlay and Cairns, 1981). Our previous work has revealed the existence of extremely effective compensatory mechanisms for neonatal target loss. This compensation occurs in part through NMDA receptor dependent regulation of retinal axon arbor size (Pallas and Finlay, 1991; Xiong et al., 1994; Razak et al., 2003) and in part through changes in lateral inhibitory circuits within SC (Pallas and Finlay, 1989; Razak and Pallas, 2003, 2007). Here we have shown that regulation of ephrin expression also occurs after damage to posterior SC. In what natural scenario would these regulatory mechanisms be important? The initial overproduction of neurons during development and the consequent mismatches in the number of projection and target cells require a flexible afferent/target matching system during development. Visual acuity depends critically on the convergence ratio between retinal ganglion cells and their target cells in the brain. The same is true during brain evolution; alterations in cell cycle number contribute to increasing brain size, in some cases altering the relative size of afferent and target populations (Finlay et al., 2001; Stevens, 2001). The ability of the ephrin-A ligand/EphA receptor system to regulate after damage illustrates how this regulatory ability could be employed in the population matching process during normal development and evolution when input and target populations are mismatched (see Pallas, 2007, for review).

These results also have important implications for clinical strategies to facilitate recovery from brain damage involving topographic projections. The ability of central sensory targets to maintain topography regardless of changes in afferent/target ratios doubtless contributes importantly to its ability to preserve stimulus tuning properties and receptive field sizes, contributing to the maintenance of function after the lesions. The mechanisms allowing the coordination of the activity-independent modulation of ephrin levels and the activity-dependent conservation of function have yet to be discovered however (Pfeiffenberger et al., 2006), and will be of great interest for future studies.

The authors are grateful to Kate Sharer and members of the Young lab for help with *in situ* hybridizations, and to the GSU Animal Care Facility for excellent animal care. The authors also thank Prof. Vincent Rehder and members of the Pallas lab for their critical comments on the article.

REFERENCES

Attardi DG, Sperry RW. 1963. Preferential selection of central pathways by regenerating optic fibers. Exp Neurol 7:46–64.

Brown APA, Yates PA, Burrola PD, Ortuno D, Vaidya A, Jessell TM, Pfaff SL, et al. 2000. Topographic mapping from the retina to the midbrain is controlled by relative but not absolute levels of epha receptor signaling. Neuron 102:77–88.

Brunet I, Weinl C, Piper M, Trembleau A, Volovitch M, Harris W, Prochiantz A, et al. 2005. The Transcription factor engrailed-2 guides retinal axons. Nature 438:94–98.

Chalupa LM, Rhoades RW. 1977. Responses of visual, somatosensory, and auditory neurons in The golden hamster's superior colliculus. J Physiol (Lond) 270:595–626.

Chen Y, Mohammadi M, Flanagan JG. 2009. Graded Levels of FGF protein span the midbrain and Can instruct graded induction and repression of neural mapping labels. Neuron 62:773–780.

Cheng HJ, Flanagan JG. 1994. Identification and cloning of ELF-1, a developmentally expressed ligand for the Mek4 and Sek receptor tyrosine kinases. Cell 79:157–168.

Cheng HJ, Nakamoto M, Bergemann AD, Flanagan JG. 1995. Complementary gradients in expression and binding of ELF-1 and Mek4 in development of the topographic retinotectal projection map. Cell 82:371–381.

Ciossek T, Monschau B, Drescher U. 1998. Eph receptor-ligand interactions are necessary for guidance of retinal ganglion cell axons in vitro. Eur J Neurosci 10:1574.

Clancy B, Darlington RB, Finlay BL. 2001. Translating developmental time across species. Neuroscience 105:7–17.

Constantine-Paton M. 1983. Position and proximity in the development of maps and stripes. Trends Neurosci 6:32–36.

Cook NL, Vink R, Donkin JJ, Van Den Heuvel C. 2009. Validation of reference genes for normalization of real-time quantitative RT-PCR data in traumatic brain injury. J Neurosci Res 87:34–41.

Danielian PS, Mcmahon AP. 1996. Engrailed-1 as a target of the wnt-1 signalling pathway in vertebrate midbrain development. Nature 383:332–334.

Davis CA, Joyner AL. 1988. Expression patterns of the homeo box-containing genes En-1 and En-2 and the proto-oncogene Int-1 diverge during mouse development. Genes Dev 2:1736–1744.

Dickinson ME, Krumlauf R, Mcmahon AP. 1994. Evidence for a mitogenic effect of Wnt-1 in the developing mammalian central nervous system. Development 120:1453–1471.

Dickinson ME, Mcmahon AP. 1992. The role of Wnt genes in vertebrate development. Curr Opin Genet Dev 2: 562–566.

Drescher U, Bonhoeffer F, Müller BK. 1997. The Eph family in retinal axon guidance. Curr Opin Neurobiol 7:75–80.

Feldheim DA, Kim YI, Bergemann AD, Frisén J, Barbacid M, Flanagan JG. 2000. Genetic analysis of ephrin-a2 and ephrin-a5 shows their requirement in multiple aspects of retinocollicular mapping. Neuron 25:563–574.

Feldheim DA, Nakamoto M, Osterfield M, Gale NW, Dechiara TM, Rohatgi R, Yancopoulos GD, et al. 2004. Loss-of-function analysis of epha receptors in retinotectal mapping. J Neurosci 24:2542–2550.

Feldheim DA, Vanderhaeghen P, Hansen MJ, Frisén J, Lu Q, Barbacid M, Flanagan JG. 1998. Topographic guidance labels in a sensory projection to the forebrain. Neuron 21:1303–1313.

Finlay BL, Cairns SJ. 1981. Relationship of aberrant retinotectal projections to visual orienting after neonatal tectal damage in hamster. Exp Neurol 72:308–317.

Finlay BL, Darlington RB, Nicastro N. 2001. Developmental structure in brain evolution. Behav Brain Sci 24:263–278; discussion 278-308.

Finlay BL, Schneps SE, Schneider GE. 1979. Orderly compression of the retinotectal projection following partial tectal ablations in the newborn hamster. Nature (London) 280:153–154.

Finlay BL, Schneps SE, Wilson KG, Schneider GE. 1978. Topography of visual and somatosensory projections to the superior colliculus of the golden hamster. Brain Res 142:223–235.

Flenniken AM, Gale NW, Yancopoulos GD, Wilkinson DG. 1996. Distinct and overlapping expression patterns of ligands for eph-related receptor tyrosine kinases during mouse embryogenesis. Dev Biol 179:382–401.

Friedman GC, O'Leary DDM. 1996. Retroviral misexpression of *engrailed* genes in the chick optic tectum perturbs the topographic targeting of retinal axons. J Neurosci 16:5498–5509.

Frisén J, Yates PA, Mclaughlin T, Friedman GC, O'Leary DDM, Barbacid M. 1998. Ephrin-A5 (AL-1/RAGS) is essential for proper retinal axon guidance and topographic mapping in the mammalian visual system. Neuron 20:235–243.

Fritzsche P, Neumann K, Nasdal K, Gattermann R. 2006. Differences in reproductive success between laboratory and wild-derived golden hamsters (*Mesocricetus auratus*) as a consequence of inbreeding. Behav Ecol Sociobiol 60:220–226.

Frost DO, So KF, Schneider GE. 1979. Postnatal development of retinal projections in Syrian hamsters: A study using autoradiographic and anterograde degeneration techniques. Neuroscience 4:1649–1677.

Frugier T, Conquest A, Mclean C, Currie P, Moses D, Goldshmit Y. 2012. Expression And activation of epha4 in the human brain after traumatic injury. J Neuropathol Exp Neurol 71:242–250.

Gattermann R, Fritzsche P, Neumann K, Al-Hussein I, Kayser A, Abiad M, Yakti R. 2000. Notes on the current distribution and the ecology of wild golden hamsters (*Mesocricetus auratus)*. J Zool Lond 254:359–365.

Gaze RM, Sharma SC. 1970. Axial differences in the reinnervation of the goldfish optic tectum by regenerating optic nerve fibers. Exp Brain Res 10:171–181.

Gebhardt C, Bastmeyer M, Weth F. 2012. Balancing of ephrin/eph forward and reverse signaling as the driving force of adaptive topographic mapping. Development 139:335–345.

Goldshmit Y, Bourne J. 2010. Upregulation of epha4 on astrocytes potentially mediates astrocytic gliosis after cortical lesion in the Marmoset monkey. J Neurotrauma 27:1321–1332.

Goodhill GJ, Richards LJ. 1999. Retinotectal maps: Molecules, models and misplaced data. Trends Neurosci 22:529–534.

Gosse NJ, Baier H. 2009. An essential role for radar (Gdf6a) in inducing dorsal fate in the zebrafish retina. Proc Natl Acad Sci USA 106:2236–2241.

Hansen MJ, Dallal GE, Flanagan JG. 2004. Retinal axon response to ephrin-as shows a graded, concentration-dependent transition from growth promotion to inhibition. Neuron 42:717–730.

Honda H. 2004. Competitive interactions between retinal ganglion axons for tectal targets explain plasticity of retinotectal projection in the servomechanism model of retinotectal mapping. Dev Growth Differ 46:425–437.

Hope RA, Hammond BJ, Gaze RM. 1976. The arrow model: Retinotectal specificity and map formation in the goldfish visual system. Proc R Soc Lond B Biol Sci 194:447–466.

Hornberger MR, Dütting D, Ciossek T, Yamada T, Handwerker C, Lang S, Weth F, et al. 1999. Modulation of epha receptor function by coexpressed ephrina ligands on retinal ganglion cell axons. Neuron 22:731–742.

Huang L, Pallas SL. 2001. NMDA antagonists in the superior colliculus prevent developmental plasticity but not visual transmission or map compression. J Neurophysiol 86:1179–1194.

Joyner AL. 1996. *Engrailed, Wnt* and *Pax* genes regulate midbrain hindbrain development. Trends Genet 12:15–20.

Joyner AL, Liu A, Millet S. 2000. Otx2, Gbx2 And Fgf8 interact to position and maintain a mid–hindbrain organizer. Curr Opin Cell Biol 12:736–741.

Knoll B, Isenmann S, Kilic E, Walkenhorst J, Engel S, Wehinger J, Bahr M, et al. 2001. Graded expression patterns of ephrin-As in the superior colliculus after lesion of the adult mouse optic nerve. Mech Dev 106:119–127.

Koulakov A, Tsigankov D. 2004. A stochastic model for retinocollicular map development. BMC Neurosci 5:30.

Lai KO, Ip FC, Ip NY. 1999. Identification and characterization of splice variants of ephrin-A3 and ephrin-A5. FEBS Lett 458:265–269.

Lemke G, Reber M. 2005. Retinotectal mapping: New insights from molecular genetics. Annu Rev Cell Dev Biol 21:551–580.

Li JYH, Joyner AL. 2001. Otx2 and Gbx2 are required for refinement and not induction of mid-hindbrain gene expression. Development 128:4979–4991.

Logan C, Wizenmann A, Drescher U, Monschau B, Bonhoeffer F, Lumsden A. 1996. Rostral optic tectum acquires caudal characteristics following ectopic *engrailed* expression. Curr Biol 6:1006–1014.

Lukehurst SS, King CE, Beazley LD, Tay DK, So KF, Rodger J. 2006. Graded ephrin-A2 expression in the developing hamster superior colliculus. Exp Brain Res 173:546–552.

Mortimer D, Pujic Z, Vaughan T, Thompson AW, Feldner J, Vetter I, Goodhill GJ. 2010. Axon guidance by growth-rate modulation. Proc Natl Acad Sci USA 107:5202–5207.

O'Leary DDM, Mclaughlin T. 2004. Mechanisms of retinotopic map development: ephs, ephrins, and spontaneous correlated retinal activity. Prog Brain Res 147:43–66.

Pallas SL. 2007. Compensatory innervation in development and evolution. In: Striedter GF, Rubenstein JLR, Striedter GF, Rubenstein J, editors. Vol. 1: Theories, Development, Invertebrates. Oxford, UK: Academic Press, pp 153–168.

Pallas SL, Finlay BL. 1989. Conservation of receptive field properties of superior colliculus cells after developmental rearrangements of retinal input. Vis Neurosci 2:121–135.

Pallas SL, Finlay BL. 1991. Compensation for population size mismatches in the hamster retinotectal system: Alterations in the organization of retinal projections. Vis Neurosci 6:271–281.

Pfeiffenberger C, Yamada J, Feldheim DA. 2006. Ephrin-As and patterned retinal activity act together in the development of topographic maps in the primary visual system. J Neuroosci 26:12873–12884.

Picker A, Brennan C, Reifers F, Clarke JD, Holder N, Brand M. 1999. Requirement for the zebrafish mid-hindbrain boundary in midbrain polarisation, mapping and confinement of the retinotectal projection. Development 126:2967–2978.

Razak KA, Huang L, Pallas SL. 2003. NMDA receptor blockade in the superior colliculus increases receptive field size without altering velocity and size tuning. J Neurophysiol 90:110–119.

Razak KA, Pallas SL. 2003. Plasticity in inhibitory circuitry maintains velocity tuning of superior collicular neurons under NMDA receptor blockade. Soc Neurosci Abstr 29:37.24.

Razak KA, Pallas SL. 2007. Inhibitory plasticity facilitates recovery of stimulus velocity tuning in the superior colliculus after chronic NMDA receptor blockade. J Neurosci 27:7275–7283.

Reber M, Burrola P, Lemke G. 2004. A relative signalling model for the formation of a topographic neural map. Nature 431:847–853.

Rodger J, Lindsey KA, Leaver SG, King CE, Dunlop SA, Beazley LD. 2001. Expression of ephrin-A2 in the superior colliculus and epha5 in the retina following optic nerve section in adult rat. Eur J Neurosci 14: 1929–1936.

Rodger J, Symonds AC, Springbett J, Shen WY, Bartlett CA, Rakoczy PE, Beazley LD, et al. 2005. Eph/ephrin expression in the adult rat visual system following localized retinal lesions: Localized and transneuronal up-regulation in the retina and superior colliculus. Eur J Neurosci 22:1840–1852.

Roelink H, Wagenaar E, Lopes Da Silva S, Nusse R. 1990. Wnt-3, a gene activated by proviral insertion in mouse mammary tumors, is homologous to Int-1/Wnt-1 and is normally expressed in mouse embryos and adult brain. Proc Natl Acad Sci USA 87:4519–4523.

Rosentreter SM, Davenport RW, Loschinger J, Huf J, Jung J, Bonhoeffer F. 1998. Response of retinal ganglion cell axons to striped linear gradients of repellent guidance molecules. J Neurobiol 37:541–562.

Rosoff WJ, Urbach JS, Esrick MA, Mcallister RG, Richards LJ, Goodhill GJ. 2004. A new chemotaxis assay shows the extreme sensitivity of axons to molecular gradients. Nat Neurosci 7:678–682.

Ruthazer ES, Cline HT. 2004. Insights into activity-dependent map formation from the retinotectal system: A middle-of-the-brain perspective. J Neurobiol 59:134–146.

Schmidt JT. 1978. Retinal fibers alter tectal positional markers during the expansion of the retinal projection in goldfish. J Comp Neurol 177:279–295.

Schmidt JT. 1982. The formation of retinotectal projections. Trends Neurosci 5:111–115.

Schmidt JT. 1983. Regeneration of the retinotectal projection following compression onto a half tectum in goldfish. J Embryol Exp Morphol 77:39–51.

Schmidt JT, Cicerone CM, Easter SS. 1978. Expansion of the half retinal projection to the tectum in goldfish: An electrophysiological and anatomical study. J Comp Neurol 177:257–278.

Schmitt AM, Shi J, Wolf AM, Lu CC, King LA, Zou Y. 2006. Wnt-Ryk signalling mediates medial-lateral retinotectal topographic mapping. Nature 439:31–37.

Schmittgen TD, Livak K. 2008. Analyzing real-time PCR data by the comparative C(T) method. Nat Protoc 3:1101–1108.

Shigetani Y, Funahashi JI, Nakamura H. 1997. En-2 regulates the expression of the ligands for eph type tyrosine kinases in chick embryonic tectum. Neurosci Res 27:211–217.

Simpson H, Goodhill G. 2011. A simple model can unify a broad range of phenomena in retinotectal map development. Biol Cybern 104:9–29.

Sperry RW. 1963. Chemoaffinity in the orderly growth of nerve fiber patterns and connections. Proc Natl Acad Sci USA 50:703–710.

Stein BE, Dixon JP. 1979. Properties of superior colliculus neurons in the golden hamster. J Comp Neurol 183:269–284.

Stevens CF. 2001. An evolutionary scaling law for the primate visual system and its basis in cortical function. Nature 411:193–195.

Sugiyama S, Funahashi J, Kitajewski J, Nakamura H. 1998. Crossregulation between En-2 and Wnt-1 in chick tectal development. Dev Growth Differ 40:157–166.

Symonds ACE, King CE, Bartlett CA, Sauve Y, Lund RD, Beazley LD, et al. 2007. Epha5 and Ephrin-A2 expression during optic nerve regeneration: A 'two-edged sword'. Eur J Neurosci 25:744–752.

Symonds ACE, Rodger J, Tan MML, Dunlop SA, Beazley LD, Harvey AR. 2001. Reinnervation of the superior colliculus delays down-regulation of ephrin A2 in neonatal rat. Exp Neurol 170:364–370.

Tiao Y-C, Blakemore C. 1976. Functional organization in the superior colliculus of the golden hamster. J Comp Neurol 168:483–504.

Triplett JW, Feldheim DA. 2012. Eph and Ephrin signaling in the formation of topographic maps. Semin Cell Dev Biol 23:7–15.

Triplett JW, Pfeiffenberger C, Yamada J, Stafford BK, Sweeney NT, Litke AM, Sher A, et al. 2011. Competition is a driving force in topographic mapping. Proc Natl Acad Sci USA 108:19060–19065.

Udin SB, Fawcett JW. 1988. Formation of topographic maps. Annu Rev Neurosci 11:289–327.

von Philipsborn AC, Lang S, Loeschinger J, Bernard A, David C, Lehnert D, Bonhoeffer F, et al. 2006. Growth cone navigation in substrate-bound ephrin gradients. Development 133:2487–2495.

Walter J, Henke-Fahle S, Bonhoeffer F. 1987. Avoidance of posterior tectal membranes by temporal retinal axons. Development 101:909–913.

Walter J, Kern-Veits B, Huf J, Stolze B, Bonhoeffer F. 1987. Recognition of position-specific properties of tectal cell membranes by retinal axons *in vitro*. Development 101:685–696.

Wikler KC, Kirn J, Windrem MS, Finlay BL. 1986. Control of cell number in the developing visual system. II. Effects of partial tectal ablation. Dev Brain Res 28: 11–21.

Wilkinson DG. 2001. Multiple roles of EPH receptors and ephrins in neural development. Nat Rev Neurosci 2: 155–164.

Wilkinson DG, Bailes JA, Mcmahon AP. 1987. Expression of the proto-oncogene Int-1 is restricted to specific neural cells in the developing mouse embryo. Cell 50:79–88.

Willshaw D. 2006. Analysis of mouse epha knockins and knockouts suggests that retinal axons programme target cells to form ordered retinotopic maps. Development 133:2705–2717.

Willshaw DJ, Von Der Malsburg C. 1979. A marker induction mechanism for the establishment of ordered neural mappings: Its application to the retinotectal problem. Philos Trans R Soc Lond B Biol Sci 287:203–243.

Xiong M, Finlay BL. 1993. Changes in synaptic density after developmental compression or expansion of retinal input to the superior colliculus. J Comp Neurol 330: 455–463.

Xiong M, Pallas SL, Lim S, Finlay BL. 1994. Regulation of retinal ganglion cell axon arbor size by target availability: Mechanisms of compression and expansion of the retinotectal projection. J Comp Neurol 344:581–597.

Yamada T, Okafuji T, Ohta K, Handwerker C, Drescher U, Tanaka H. 2001. Analysis of ephrin-A2 in the chick retinotectal projection using a function-blocking monoclonal antibody. J Neurobiol 47:245–254.

Yoon MG. 1976. Progress of topographic regulation of the visual projection in the halved optic tectum of adult goldfish. J Physiol 257:621–643.